HHS Public Access

Author manuscript

J Autoimmun. Author manuscript; available in PMC 2016 January 07.

Published in final edited form as:

J Autoimmun. 2014 September ; 53: 10–25. doi:10.1016/j.jaut.2014.07.001.

Compromised central tolerance of ICA69 induces multiple organ autoimmunity

Yong Fan[a,1], **Giulio Gualtierotti**[a], **Asako Tajima**[a,1], **Maria Grupillo**[a], **Antonina Coppola**[a,2], **Jing He**[a], **Suzanne Bertera**[a,1], **Gregory Owens**[a,3], **Massimo Pietropaolo**[b], **William A. Rudert**[a,1], and **Massimo Trucco**[a,1,*]

[a]Division of Immunogenetics, Department of Pediatrics, University of Pittsburgh School of Medicine, Pittsburgh, PA, USA

[b]Department of Medicine, University of Michigan Medical School, Ann Arbor, MI, USA

Abstract

For reasons not fully understood, patients with an organ-specific autoimmune disease have increased risks of developing autoimmune responses against other organs/tissues. We identified ICA69, a known β-cell autoantigen in Type 1 diabetes, as a potential common target in multi-organ autoimmunity. NOD mice immunized with ICA69 polypeptides exhibited exacerbated inflammation not only in the islets, but also in the salivary glands. To further investigate ICA69 autoimmunity, two genetically modified mouse lines were generated to modulate thymic ICA69 expression: the heterozygous ICA69$^{del/wt}$ line and the thymic medullary epithelial cell-specific deletion Aire-ΔICA69 line. Suboptimal central negative selection of ICA69-reactive T-cells was observed in both lines. Aire-ΔICA69 mice spontaneously developed coincident autoimmune responses to the pancreas, the salivary glands, the thyroid, and the stomach. Our findings establish a direct link between compromised thymic ICA69 expression and autoimmunity against multiple ICA69-expressing organs, and identify a potential novel mechanism for the development of multi-organ autoimmune diseases.

Keywords

ICA69; Thymus; Primary Sjogren's syndrome; Autoimmune thyroiditis; Autoimmune diabetes; Autoimmune polyendocrine syndrome

[*]Corresponding author. Institute of Cellular Therapeutics, Allegheny Health Network, 320 East North Avenue, 11th Floor, South Tower, Pittsburgh, 15212, PA, USA. MTrucco1@wpahs.org, mnt@pitt.edu (M. Trucco).

[1]Current address: Institute of Cellular Therapeutics, Allegheny Health Network, Pittsburgh, PA, USA.

[2]Current address: Section of Endocrinology, Dipartimento Biomedico di Medicina Interna e Specialistica (DIBIMIS), University of Palermo, Palermo, Italy.

[3]Current address: Peace Health Southwest Medical Center, Vancouver, WA, USA.

Author contributions

Y.F. and M.T. conceived the project, planned the experiments, and wrote the manuscript. Y.F., G.G., A.T., M.G., A.C., J.H., S.B., and G.O. performed the experiments. W.A.R. and M.P. provided intellectual input and edited the manuscript.

Competing interests

The authors declare that they have no competing interests.

Appendix A. Supplementary information

Supplementary information associated with this article can be found, in the online version, at http://dx.doi.org/10.1016/j.jaut.2014.07.001.

1. Introduction

Patients with organ-specific autoimmune diseases, such as Type 1 diabetes (T1D) [1], have increased propensity for developing autoimmune disorders targeting other organs and tissues. About 25–40% of T1D patients develop autoantibodies against thyroid proteins (e.g. thyroglobulin and thyroid peroxidase) commonly associated with autoimmune thyroid disease and some eventually display clinical symptoms [2,3]. A better understanding of this clustering phenomenon of autoimmune disorders is important for full spectrum clinical care of these patients [4,5].

While key immune modulating genes (e.g. MHCs and CTLA-4) have been implicated in the comorbidity of autoimmune disorders, recent studies of autoimmune polyendocrine syndrome 1 (APS1) have highlighted another potential mechanism underlying the failure of immune tolerance to multiple organs. APS is a collective group of autoimmune disorders characterized by the involvement of two or more endocrine and/or exocrine glands [6,7]. Based on the affected organs and the age of disease onset, APS are divided into the very rare juvenile type APS1, and the relatively common types, including APS2 (with Addison's disease [AD]) and APS3 (without AD). It is well-established that mutations within the autoimmune regulator (*Aire*) gene are the primary cause of APS1 [8,9]. AIRE regulates the expression of a broad range of peripheral tissue-specific antigens (TSAs) in medullary thymic epithelial cells (mTECs). Mutation in the Aire gene results in significant decrease of TSA expression in the thymus, leading to autoimmune responses to multiple organs and tissues [10–12]. These studies clearly demonstrate that thymic TSAs play a pivotal role in defining the molecular identities of peripheral tissues within the thymus medulla, and therefore facilitate the negative selection of tissue-specific autoreactive T cells. The underlining molecular causes for APS2 and APS3 (collectively designated as APS 2&3 hereinafter) are still not fully understood.

Islet autoantigen 69 (ICA69), encoded by the *Ica1* gene, was first identified by screening a human islet cDNA expression library with serum samples harvested from 1st degree relatives of T1D patients, who also displayed islet seroreactivity and progressed to overt T1D later in their life [13–15]. Unlike insulin and other β-cell specific islet autoantigens [16–18], ICA69 is also present in a wide range of extrapancreatic endocrine and exocrine tissues (e.g. the thyroid, the salivary glands, the brain, the stomach, and the testis). Although its physiological function is not fully known, recent studies suggest that ICA69 might be a key regulator of the biogenesis of secretory vesicles in endocrine/exocrine cells [19,20].

Similar to insulin and other tissue-specific antigens, ICA69 is also ectopically expressed in mTECs [21–24]. Interestingly, the level of *Ica1* mRNA transcript in the thymus is significantly decreased in the T1D-prone non-obese diabetes (NOD) mouse strain, in comparison to that of the T1D-resistant C57BL/6 strain, suggesting that failure of negative selection of ICA69-specific thymocyte is one of the driving forces in autimmunity progression in NOD mice [22,23,25].

Anti-ICA69 immune reactivity has also been implicated in primary Sjogren's syndrome (PSS), an autoimmune disease affecting the salivary and lacrimal glands [26]. In comparison

to their wild-type counterparts, NOD mice with impaired global expression of the N-terminal, first coding exon of the *Ica1* gene had lower severity of sialadenitis, suggesting an antigenic role for ICA69 in eliciting immune responses to the salivary glands [26–28]. More recently, *Ica1* was identified as a potential susceptibility locus of systemic lupus erythematosus in genetic association studies [29]. All these observations suggest that anti-ICA69 immune reactivity might be a common contributing factor to the progression of overlapping but physiologically distinct autoimmune disorders.

Here, we show that immune reactivity to ICA69 is sufficient to initiate and propagate inflammation inside multiple ICA69-expressing glands. Thymic deletion of ICA69 expression, even on the autoimmune resistant C57BL/6 genetic background, is sufficient to induce inflammation inside multiple organs. Our findings high-light a potential role for ICA69 as a target in multi-organ autoimmune disorders, in addition to its implication in T1D.

2. Materials and methods

2.1. Mice

All animal protocols were reviewed and approved by the University of Pittsburgh Institutional Animal Care and Use Committee. NOD/Ltj and C57BL/6 mice were purchased from the Jackson Laboratory (Bar Harbor, ME). Only female NOD/Ltj mice were used in the study. Mice with two loxp sites genetically engineered to flank exon 14 of the *Ica1* gene (floxed) were generated through standard gene targeting methods as previously described [24,30]. Detailed procedures for assembling the Ica1 exon 14 targeting construct used in the study are available upon request. Heterozygous $ICA^{flox/wt}$ mice were backcrossed to C57BL/6 mice for five generations before intercross to obtain the homozygous $ICA^{flox/flox}$. To generate the Aire-ΔICA69 line, $ICA^{flox/flox}$ mice were crossed to the Aire-Cre transgenic mice [24], developed in our laboratory. To generate the $ICA^{del/wt}$ line, $ICA^{flox/wt}$ mice were first crossed to B6.CMV–Cre transgenic mice to obtain the $Ica1^{del}$ allele in the germline, followed by further backcrossing to C57BL/6 mice to breed out the CMV-Cre transgene (Jackson Laboratory). Of note, all the *Ica1* genetically modified mouse lines used in this study (i.e., $ICA^{del/wt}$, $ICA^{flox/flox}$ and Aire-ΔICA69) are on the B6 genetic background.

2.2. ELISPOT

ELISPOT was performed using the BD mouse IFN-γ Set, according to the manufacturer's specifications (BD Biosciences). Splenocytes (1×10^6 unless specified otherwise) were cultured overnight (unless specified otherwise), with ICA69 peptides (10 μg/ml). Assays were performed in triplicate and averaged. The assays were repeated at least three times.

2.3. Genotyping of the genetically modified mice

0.5 cm tail biopsies were surgically removed from 14 to 20 day old pups. Genomic DNA was isolated with DNeasy Blood and Tissue Kit (Qiagen Inc., Valencia, CA). The following primer pairs were used for genotyping: Aire-Cre (5′-GAGTGATGAGGTTCGCAAGAA-3′ and 5′-GCGCGCCTGAAGATATAGAAG-3′); $Ica1^{flox}$ allele (5′-TCAGCATGTTTGAGA ATCACAAGA-3′ and 5′-CTTATAGAGAAGCCAAGTATTGGA-3′).

2.4. Blood glucose measurement and intraperitoneal glucose tolerance test (IPGTT)

Blood glucose levels were measured with the Ascensia Contour blood glucose monitoring system (Bayer HealthCare LLC, Mishawaka, IN). To perform IPGTT, mice were fasted overnight (~16 h) and injected intraperitoneally with a bolus of 2 g of D-glucose (Sigma–Aldrich, St. Louis, USA) per kilogram of body weight. Blood was sampled from a small nick of the tail-vein at 0, 15, 30, 60, 90 and 120 min after glucose injection.

2.5. RNA analysis

The total RNA of spleens or thymi was isolated using an RNA minikit, according to the manufacturer's protocol (Qiagen). Following DNase I treatment (Ambion), RNA samples were reverse-transcribed into cDNAs with Superscript III cDNA kit, (Invitrogen). qPCR analyses of gene expression in cDNA samples in Figs. 2A and 3A were performed with the LightCycler FastStart DNA Master SYBR Green I kit, and analyzed with the LightCycler 2 software (Roche Applied Science). The following primers were used for Ica1 (F 5′-TGAGTCTGCAACCTTCAACAGGGA-3′, R 5′-AAACAGGGCCTTGACCCTCTCATT-3′); Hprt (F 5′-GGATACAGGCCAGACTTTGTTGGA-3′, R 5′ -CAACAGGACTCCTCGTATTTGCAG-3′); Ins (F 5′-AGATGCGTT TAAGGTTCGACTG-3′, R 5′-TATCAGATGTGCCCACTAACAC-3′). To absolute number of mRNA transcripts of Ica1 were obtained with TaqMan qPCR assay with ABI 7900HT Real-time PCR machine, and normalized to the absolute numbers of 18S. The following primer and probe sets were used: Ica1 (F 5′-AAAGATCTCCAGGCCTCTCT-3′, R 5′-CAACAGCATCAGGGTTTGATAAG-3′, probe, 5′ FAMTGACTGCCTGGTTCAGCCTCTTT-Tamara 3′); 18S (F 5′-CACGGACAGGATTGACAGATT-3′, R 5′ –GCCAGAGTCTCGTTCGTTATC-3′, probe 5′ FAM-AGTTGGTGGAGCGATTTGTCTGGT-Tamara 3′). Isolated PCR products of Ica1 or 18S cDNA fragments were quantified by spectrometer, serial diluted and were used as templates to generate standard curves.

2.6. Histology and immunohistochemistry

Pancreas, liver, stomach, salivary glands, heart, kidney, thyroid gland, thymus and all the other organs were harvested, fixed in 4% paraformaldehyde for 3 h at 4 °C, and placed in 30% sucrose overnight. Cryosections of 5 μm thick were cut and stained with primary antibodies. Antibodies used in the study: B220, CD45, CD4 and CD8 (BD Biosciences, Franklin Lakes, NJ); Insulin (Santa Cruz Biotechnology, Santa Cruz, CA); Glucagon (Zymed, San Francisco, CA); Epcam (rat anti-mouse CD326 clone G8.8, 1:30, BD Biosciences; or polyclonal rabbit anti-Epcam antibody, 1:100, ABBIO-TEC). EGFP (Chicken anti-GFP primary antibody, 1:100, Abcam). Ulex Europaeus Lectin 1 (Rabbit polyclonal to UEA-1, Abcam).

2.7. Flow cytometry

Flow cytometric analysis was performed on the BD FACSCalibur flow cytometer (BD Biosciences, San Jose, CA) and analyzed with CellQuest Pro software (BD Biosciences). Single cell suspensions were prepared from spleen, subjected to erythrocyte depletion in red

blood cell lysis buffer (Sigma–Aldrich, St. Louis, MO), blocked with anti-CD16/32 antibody and then stained with the other antibodies. The following antibodies were purchased from BD Biosciences: anti-CD16/32 (2.4G2), anti-CD4 PeCy5 (H129.9), anti-CD45-APC (30-F11), and anti-CD3-APC (145-2C11). Anti-CD25-APC (7D4) antibody was purchased from Miltenyi Biotec (Auburn, CA). Staining buffer: phosphate buffered saline (PBS, calcium and magnesium free, Invitrogen) supplemented with 1% bovine serum albumin (BSA, Sigma–Aldrich) and 0.1% sodium azide (Sigma–Aldrich). Intracellular staining of the Foxp3 protein was performed with commercial kit purchased from eBiosciences (San Diego, CA), following manufacturer's suggested protocol.

2.8. Anti-exon 14 and anti-TG autoantibody assay

A 96-well EIA plate was coated with 0.1 μg of ICA69 exon 14 polypeptide or human thyroglobulin (Prospec-Tany Tecnogene Ltd., East Brunswick, NJ) in 100 μl of PBS at 4 °C overnight. Wells were blocked with PBS with 10% BSA for 2 h at room temperature, and probed with mouse sera collected from naïve or immunized mice and age-matched controls (1:00 dilution, 100 μl in each well) for another 2 h. Next, biotin-conjugated rat anti-mouse IgG (BD Biosciencs) was added to the well (1:15,000 dilution) and incubated for 60 min, followed by incubation with horseradish peroxidase (HRP) conjugated streptavidin (1:4000) for 30 min. Lastly, TMB substrate (BioLegned, San Diego, CA) was added to each well and the absorbance was measured at 450 nm (minus 570 nm for wavelength correction) with microplate reader (Molecular Devices).

2.9. Measurement of the saliva flow rate (SFR)

To evaluate the secretory function of the salivary glands (saliva flow rate, SFR), mice were anesthetized with intraperitoneal injection of Avertin (Sigma, 250 mg/kg body weight), followed by subcutaneous injection of pilocarpine hydrochloride (Sigma, at 0.5 mg/kg body weight) as stimulant for secretion. Whole saliva was collected from the oral cavity using micropipette at 10, 20 and 30 min after pilocarpine injection. The SFR is calculated by the weight (mg) of the saliva/min/bodyweight.

2.10. Histological assessment of salivary gland and pancreas inflammation

The submandibular salivary glands of NOD mice were fixed in formalin, embedded in paraffin and cut in 5 μm sections. Four to five sections (each about 100 μm from the previous) were mounted on glass slides, stained with hematoxylin and eosin (H&E) and evaluated by two different examiners. One lymphocytic focus is defined as an aggregate of >50 infiltrates. The focus score (FS) is determined by the number of foci per mm^2 [31,32]. The pancreata of NOD mice were collected, processed and stained similar to the salivary gland. A total of approximately 100 islets from 5 animals were assessed by two different examiners.

2.11. Statistical analysis

All values are expressed as the mean ± s.e.m. unless otherwise specified. In mouse studies, statistical significance was determined using unpaired, Student *t* test. For analysis of results from thyroid hormone and gastrin levels in mouse sera, the Mann–Whitney *U* test was

performed. The Kaplan–Meier log rank statistical test was performed to determine the statistical significance in diabetes incidence among the E14 immunized NOD mice. All statistical analyses were carried out with the GraphPad Prism 4.0 Software. In all experiments, differences were considered significant when p was less than 0.05.

3. Results

3.1. Acceleration of diabetes progression in NOD mice immunized with the ICA69 C-terminal peptide

To investigate the role of anti-ICA69 immune reactivity in the development of T1D and other coincident autoimmune disorders, we immunized 8-week old, prediabetic female NOD mice with an ICA69 C-terminal polypeptide. We focused on the C-terminal region of the ICA69 protein in this study, since our *in silico* analysis identified a conserved stretch of 39 amino acids encoded by the last exon (exon 14, designated as E14 hereinafter) that displays 100% homology between mouse and human (Fig. 1A). In addition, immune-epitope predicting software (e.g. SYFPEITHI) suggested that E14 contains motifs of T-cell epitopes that can be presented by various alleles of mouse and human MHC molecules [33,34].

High titers of antibodies against E14 were detected 4 weeks post-immunization, indicating that the vaccination promoted humoral responses against ICA69 (Fig. 1B). In addition, ELISPOT analyses of splenocytes harvested from the E14-immunized mice demonstrated the presence of a population of interferon-γ (IFNγ) producing, ICA69-reactive T-cells (Fig. 1C).

Pancreatic histology showed that as early as 4-weeks post immunization, E14-treated NOD mice developed more severe insulitis than controls, suggesting an antigenic role of E14 in islet inflammation (Fig. 1D). Interestingly, a significant concurrent decrease of $CD4^+Foxp3^+$ regulatory T cells (T_{reg}) was also observed in the pancreatic lymph nodes of E14-immunized mice 4-weeks post-immunization (Fig. 1E, *left* panel). Notably, no numerical difference of Tregs was found between the E14 immunized mice and CFA controls. In contrast, we observed an increase of the absolute numbers of total T-cells in the PLNs of E14-immunized mice, in comparison to those of the CFA-treated controls. Thus, the decrease of the percentages of Tregs in the PLNs is more likely attributed to the uncontrolled expansion of ICA69-reactive effector T cells in PLNs, not because of loss of Tregs.

To further determine if anti-E14 immune response leads to acceleration of islet destruction, we immunized another cohort of 8-week old female NOD mice with E14 and monitored their diabetes progression. Previous studies have shown that NOD mice immunized with complete Freund's adjuvant (CFA) alone have a markedly reduced incidence of diabetes than untreated NODs, and that this reduced incidence is associated with a decrease in the number of β cell-specific, autoreactive, cytotoxic T lymphocytes (CTL) [35]. We hypothesized that while E14 vaccination could promote the proliferation of E14-reactive T cells, the presence of CFA in the regimen might impair the immune responses against other β cell autoantigens. This would enable us to specifically evaluate the antigenic role of E14 in islet destruction and diabetes progression in NOD mice. Indeed, a significant acceleration of

diabetes progression was observed in cohorts of E14-immunized NOD mice, in comparison to CFA controls (Fig. 1F).

3.2. Progression of autoimmune sialadenitis in NOD mice immunized with E14 polypeptides

We have previously found high levels of steady-state *Ica1* mRNA transcripts in the pancreatic islets, as well as in two immune privileged organs, the brain and the testis [13,36]. To investigate the role of ICA69 in mediating autoimmunity against extrapancreatic organs, we first compared the levels of *Ica1* mRNA transcripts in various mouse tissues by RT-qPCR analysis, to identify the potential targets. It was found at moderate levels in the salivary glands, the stomach and other neuroendocrine tissues and organs (Fig. 2A).

Next, we examined whether E14 immunization could induce inflammation in salivary glands, which display the secondary highest levels of *Ica1* transcripts among non-immune privileged organs. In addition to T1D, NOD mice spontaneously develop autoimmune exocrinopathy and have been used as an experimental model to study the pathogenesis of primary Sjogren's syndrome (PSS) [37–39]. Moreover, ICA69 was implicated as a self Ag in PSS [26]. A major histological hallmark of PSS is the formation of lymphocyte foci (clustered lymphocytic infiltrates) in the salivary glands, which increase in number and size with disease progression. We found that NOD mice vaccinated with E14 emulsified in CFA had significant higher focus scores (FS) than controls treated with CFA alone (Fig. 2B and C), in conjunction with a higher percentage of areas with infiltrates (Fig. 2D). These results are consistent with a potential antigenic role of C-terminal ICA69 polypeptides in PSS etiology.

3.3. Correlation between diminished thymic ICA69 expression and increased peripheral anti-ICA69 immune reactivity

Similar to insulin, ICA69 is also expressed in the thymus and its level of expression is significantly decreased in NOD mice, in comparison to that of diabetes-resistant C57BL/6 mice [22,23]. To unravel the underlying mechanism(s) of ICA69 in mediating multi-organ autoimmunity and to elucidate the immunologic role of thymic ICA69 expression, we generated heterozygous *Ica1* deficient mice ($ICA^{del/wt}$), in which one copy of the mouse *Ica1* gene is systemically eliminated (Supplementary Fig. S1). Our primary goals were to examine whether the level of thymic ICA69 expression is, like insulin, copy-number dependent [40], and whether there exists a causative relationship between low levels of thymic ICA69 expression and peripheral anti-ICA69 immune reactivity. Mice homozygous for *Ica1*-deletion ($ICA^{del/del}$) would not be useful since the expression of ICA69 would also be completely abolished in the peripheral organs. Deleting one copy of the Ica1 gene resulted in a significant decrease of levels of full-length Ica1 mRNA transcripts in CD45- thymic stromal cells (Fig. 3A). We also performed TaqMan qRT-PCR analyses to compare, quantitatively, the levels of mRNA transcription between the $ICA^{del/wt}$ mice and wild-type control mice in extrathymic tissues and organs. While a general decrease was observed, substantial levels of Ica1 mRNA transcripts were retained in all the organs examined (Fig. 3B). ICA69-immunoreactive T-cells were detected in the spleens of $ICA69^{del/wt}$ mice, but

not in wild-type littermate controls by ELISPOT when peptides derived from the C-terminal half of the ICA69 protein were used as immunogens (Fig. 3C).

Only a small number of islets were found infiltrated with lymphocytes in ICA69$^{del/wt}$ pancreata (representative affected islets shown in Fig. 3G). In these mice, the relatively normal pancreatic expression of ICA69 suggests that ICA69 epitopes are not readily exposed to autoreactive T cells under the non-autoimmune environment of C57BL/6 mice. To study the interaction between the ICA69 protein expression in the islet β cells and ICA69-reactive T-cells, we transplanted wildtype (ICA69$^{wt/wt}$) islets underneath the kidney capsule of ICA69$^{del/del}$ mice and examined the infiltration of immune cells with immunohistochemistry three months later. No insulitis was observed (data not shown), further suggesting that in the absence of inflammation and genetic susceptibility to autoimmunity, epitopes derived from the islets are ineffectively presented, thus promoting a minimal expansion of ICA69-specific T-cells.

To further investigate the role of anti-ICA69 immune reactivity, we immunized ICA69$^{del/wt}$ mice with the E14 polypeptide. High titers of autoantibodies against E14 were detected in the sera of both immunized ICA69$^{del/wt}$ mice and control wildtype mice (Supplementary Fig. S2). In addition, E14 peptide-specific, IFNγ-producing T-cells were found in the spleens of ICA69$^{del/wt}$ mice four months after the initial immunization, suggesting the presence of persistent anti-ICA69 immune reactivity (Fig. 3D). E14-immunized ICA69$^{del/wt}$ mice displayed defects in maintaining glucose homeostasis upon intraperitoneal glucose challenge (Fig. 3E), in conjunction with reduced serum insulin concentrations (Fig. 3F). In contrast to the sporadic, mild insulitis observed in the immunized wild-type B6 mice and naïve ICA69$^{del/wt}$ mice, insulitis in pancreata of immunized ICA69$^{del/wt}$ mice was more prevalent and severe (Fig. 3G). These results suggested that immunization with the E14 peptide can effectively exacerbate the anti-islet autoimmune responses in ICA69$^{del/wt}$ mice, presumably attributable to the expansion of recently generated or preexisting E14-specific autoreactive T-cells that escaped thymic negative selection. Thus, anti-ICA69 autoimmunity derived from faulty negative selection of E14-reactive T-cells may play a role in exacerbating islet autoimmunity and accelerating T1D disease progression.

3.4. Development of autoimmune responses against multiple endocrine glands in E14-immunized ICA$^{del/wt}$ mice

Immunohistochemistry performed on tissues harvested from immunized ICA69$^{del/wt}$ mice revealed immune cell infiltration in tissues with relatively high levels of ICA69 expression, including the salivary glands and the stomach, whereas no accumulation was observed in organs with low levels of ICA69 expression, such as the liver and the heart (Fig. 4A and Supplementary Fig. S3). To evaluate the pathological impacts of lymphocytic infiltration to the functions of the salivary glands and the stomach, we measured the saliva flow rates and serum gastrin levels, respectively. In both cases, no significant difference was observed between the wildtype controls and the ICA$^{del/wt}$ mice (Supplementary Fig. S4).

Notably, the organ with the most significant immune cell infiltration was the thyroid (Fig. 4B). Although young ICA$^{del/wt}$ mice did not display any obvious clinical symptoms of hypothyroidism (i.e. dry hair, water retention and weight gain), low plasma concentrations

of triiodothyronine (T3) were detected. A small, but non-significant elevation of thyroid-stimulating hormone (TSH) levels was also observed (Fig. 4C). These results suggested that E14-immunized ICA$^{del/wt}$ mice developed subclinical hypothyroidism that is commonly present in patients with autoimmune disorders.

Autoimmune thyroid disease (AITD), such as Hashimoto's thyroiditis, often manifests as humoral and/or cellular immune reactivity against thyroid proteins, such as thyroid peroxidase (TPO) and thyroglobulin (TG) [41,42]. Although anti-TG autoantibody titers in the majority of the animals were close to the background levels, a small percentage of immunized ICA$^{del/wt}$ mice developed anti-TG autoantibodies spontaneously (Supplementary Fig. S5A). Interestingly, IFNγ-producing, TG-specific autoreactive T-cells were more prevalently detected in the spleens of immunized ICA69$^{del/wt}$ mice (Supplementary Fig. S5B). This cellular anti-TG reactivity suggests that the anti-ICA69 autoimmunity in ICA69$^{del/wt}$ mice could underlie the damage of the thyroid tissue, eventually resulting in clinically manifest autoimmune thyroiditis.

3.5. Induction of autoimmune responses to multiple endocrine/exocrine glands by thymic specific deletion of the ICA69

To further understand the implications of ICA69-expression in mTECs, we crossed female B6.ICA69$^{flox/flox}$ mice (Supplementary Fig. S1) to male B6.Aire-Cre transgenic mice to generate the Aire-ΔICA69 animal strain. We have shown previously in the ID-TEC animal model (for insulin deletion specifically in medullary thymic epithelial cells) that the Aire-Cre transgene can mediate the deletion of the floxed mouse *Ins2* gene specifically in the Aire-expressing mTECs, while leaving it largely intact in the pancreatic islets [24]. Similarly, transcription of the Ica1 gene was predominantly abrogated in the thymic stroma (Fig. 5A and B). In contrast, its transcription in pancreatic islets and other peripheral tissues and organs (i.e. thyroid glands, salivary glands, liver, and stomach) was largely retained (Fig. 5C). Western blot analyses further demonstrated the expression of ICA69 protein in extrathymic tissues and organs of the Aire-ΔICA69 mice (Fig. 5D). Immunohistochemical analysis of thymic sections of Aire-ΔICA69 mice showed efficient deletion of the ICA69 protein in mTECs (Fig. 5E).

ELISPOT revealed the spontaneous development/expansion of E14-reactive T-cells in the spleens of Aire-ΔICA69 mice (Fig. 5F). Both TH1- and TH2-polarized T-cells, producing IFNγ and IL-4/IL-10 cytokines, respectively, upon on E14 exposure, were detected. We also examined the composition of CD4+Foxp3+ Tregs in the spleen, the pancreatic lymph nodes and the mesenteric lymph nodes. No significant difference was observed between the Aire-ΔICA69 mice and the controls (Supplementary Fig. S6).

As early as 12-weeks of age, Aire-ΔICA69 mice displayed abnormalities in intraperitoneal glucose tolerance test (Fig. 6A). Impairment of insulin secretion upon glucose stimulation was also observed (Fig. 6B), concurrent with immune cell accumulated around the affected islets (Fig. 6C). Of note, even at 8 months of age, Aire-ΔICA69 mice remained euglycemic without glucose challenge (data not shown), suggesting that anti-ICA69 autoimmunity *per se* is not sufficient to lead to the destruction of a critical mass of pancreatic β-cells to result in clinical hyperglycemia in the diabetes-resistant B6 genetic background.

In addition to insulitis, Aire-ΔICA69 mice also spontaneously developed severe sialadenitis (Fig.7A and B), consistent with previous studies implicating ICA69 as a potential autoantigen for PSS [26]. Compromised salivary gland function was observed in these animals, and was manifested by a decreased saliva secretion rate upon stimulation and as reduced protein concentrations in the saliva (Fig. 7C and D). Furthermore, Aire-ΔICA69 mice displayed a further gradual decline of saliva secretion with age (Fig. 7E), indicating the chronic progression of PSS in these mice. These results suggest that ICA69 is a potentially important autoantigen in the development of PSS.

Immune cell infiltration was also observed in the thyroid glands (Fig. 8A). Both CD4+ and CD8+ T-cells were found, but not B220+ B-cells (Fig. 8A). In addition, CD4+ T-cells were found to infiltrate the stomach (Fig. 8B). Consistently, a mild but significant decrease of serum gastrin levels was observed in Aire-ICA69 mice, in comparison to controls (Fig. 8C).

To further demonstrate the essential roles of *Ica1* expression in mTECs in mediating ICA69-specific immune tolerance, we performed thymus-transplantation experiments. ICA69$^{del/del}$ thymi were transplanted underneath the kidney capsules of athymic nude mice, which retained normal *Ica1* expression in the peripheral lymphoid organs. While normal levels of T-regulatory cells were observed in the reconstituted mice (data not shown), T-cell infiltration into endocrine/exocrine glands (e.g. the pancreas, the salivary glands and the stomach) was observed in the thymus-transplanted nude mice, with similar patterns observed in Aire-ΔICA69 mice (Fig. 9A). Thus, defective thymic ICA69 expression seems to be sufficient *per se* to induce the T-cell mediated multi-organ autoimmune responses.

To investigate the role of thymic ICA69 expression in APCs of hematopoietic origin in the negative selection of ICA69-specific autoreactive T-cells, myeloablated C57BL/6 mice were reconstituted with ICA69$^{del/del}$ bone marrow. No immune cell infiltration in ICA69-expressing organs was observed. Furthermore, ELISPOT with ICA69 exon 13 and exon 14 encoded peptides as stimuli showed only background levels of ICA69-reactive T-cells, as compared with controls. These results suggest that ICA69 expression in Aire^{+} CD45^{-} thymic stromal cells plays a dominant role in mediating negative selection of ICA69-specific autoreactive T-cells, and in the establishment of the immune tolerance to ICA69-expressing organs.

3.6. Role of anti-ICA69 specific T-cells in multiple organ autoimmunity in Aire-ΔICA69 mice

In most of the affected organs in ICA69$^{del/wt}$ and Aire-ΔICA69 mice, infiltration by both CD4^{+} and CD8^{+} T-cells was observed, suggesting a major role for ICA69-specific T-cells in mediating multiple organ/tissue autoimmunity. To demonstrate that ICA69-specific autoreactive T-cells were sufficient to induce autoimmune responses in the various ICA69-expressing organs, adoptive T-cell transfer experiments were performed, in which T-cells harvested from the spleens of Aire-ΔICA69 mice were intravenously injected into immune deficient Rag1$^{-/-}$ mice. Four weeks after the T-cell transfer, immunohistochemical analyses revealed infiltration of T-cells into multiple ICA69-expressing organs, including the thyroid, salivary glands and parotid glands, whereas none was observed in recipients injected with control T-cells (Fig. 9B). These results further suggest that ICA69-specific autoreactive T-cells were responsible for the multiple organ autoimmunity observed in Aire-ΔICA69 mice.

4. Discussion

The role of anti-ICA69 autoimmunity in T1D progression has long been underappreciated, perhaps because the current radio-immunoassay targeting the full-length of ICA69 protein has yet to achieve the same levels of efficacy to reliably distinguish diabetic sera from controls unlike assays for other autoantigens (e.g. Insulin, GAD65, Znt8 and IA2) [43–46]. Notably, in both the Aire-ΔICA69 and ICA69$^{del/wt}$ mouse strains, cellular immune responses mediated by anti-ICA69 autoreactive T-cells, rather than autoantibody responses, predominate. This might be the explanation why, compared to other autoantibodies, anti-ICA69 autoantibodies may not be clinically significant markers for T1D prediction. Nevertheless, both Aire-ΔICA69 mice and ICA69 E14-immunized ICA69$^{del/wt}$ mice displayed impaired insulin secretion and glucose intolerance upon intraperitoneal glucose challenge, suggesting a contributory role of anti-ICA69 autoimmunity in islet destruction. In contrast with our previously described thymic specific insulin-deleted B6.ID-TEC animal model, which fully develops clinical diabetes three weeks after birth [24,47], these animals did not develop overt diabetes. These data, in conjunction with the observation that ICA69 + islets were not destroyed when transplanted into the ICA69-deficient mice, suggest that anti-ICA69 autoimmunity might not be the primary factor for the initiation of islet destruction in T1D. Rather, islet damage inflicted by autoreactive T-cells against primary autoantigens (e.g., insulin) might facilitate/trigger anti-ICA69 autoimmune responses in susceptible individuals, resulting in the propagation of ICA69-specific autoreactive T cells, which could subsequently drive inflammation in other ICA69-expressing exocrine and endocrine glands (e.g., salivary glands and thyroid).

The observation that no obvious lymphocytic infiltration and destruction was observed in ICA69 + wild type islets transplanted into the ICA69-deficient mice, whereas insulitis developed simultaneously in Aire-ΔICA69 mice, deems further discussion. In both cases, thymic ICA69 expression is abrogated, resulting in the release of ICA69-reactive T-cells in the periphery. There are a number of potential explanations for this discrepant outcome. First, unlike insulin undergoing pulsatile secretion, ICA69 is an intracellular, perimembrane protein. Without tissue damage and/or developmental restructure, epitopes from ICA69 are not released to the extracellular environment, to be phagocytosized and presented by professional antigen presenting cells (APCs). Therefore, ICA69 epitopes from the wild type islets transplanted under the kidney capsules of the ICA69 knockout mice were not necessarily being presented to APCs to promote inflammatory responses. In addition, ICA69-reactive T-cells in the ICA69 knockout mice were not able to expand in the periphery due to the absence of ICA69 antigens. In contrast, previous studies have shown that during the second and third week of postnatal life, neonatal pups develop excessive β-cell apoptosis [48,49]. The shedding of islet antigens through the apoptotic process might be able to activate APCs, and promote the proliferation and homing of ICA69-reactive T-cells in Aire-ΔICA69 pups. Second, the presence of islet antigen-reactive T-cells in secondary lymphoid organs does not necessarily translate into inflammatory reaction to the islets. Development of effector T-cells precedes that of Treg cells in neonatal pups [50]. Previous studies have shown that a proper Teff/Treg ratio at the neonatal stage is pivotal to establish peripheral self-tolerance. Indeed, delay of Treg migration from the thymus via thymectomy

at day 3, has been associated with organ-specific autoimmune disease [51]. Thus, proliferation of the initial wave of ICA69-reactive effector T-cells could disturb the proper ratio of Teff/Treg cells, leading to homing and expansion of ICA69-reactive effector T-cells in the islets. In contrast, the Treg population in the ICA69 knockout mice would be sufficient to prevent the expansion of ICA69-reactive Teff cells even when they were exposed to ICA69 + islet grafts.

Previous studies suggested the existence of antigenic mimicry between the immunodominant ABBOS region of bovine serum albumin (BSA, aa 152–169) and the Tep69 peptides of human ICA69 (aa 36–47 of the N-terminal region, encoded by exon 2 of the ICA1 gene) [13,52,53]. Immunization of NOD mice with BSA generates cross-reactive T-cell responses to both Tep69 and ABBOS. Accordingly, exposure to BSA or other bovine products could promote autoimmune responses against ICA69 through molecular mimicry, which might, in turn, induce mild inflammation in ICA69-expressing exocrine/endocrine glands, and become persistently present in genetically susceptible, but otherwise healthy animals. All these observations imply that immune responses against the N-terminal ICA69 region might be fairly prevalent in the general population. In contrast to the previous findings [54], our analysis of T1D patients who developed autoimmune disorders of extrapancreatic endocrine/exocrine tissue(s) showed immune reactivity to the highly conserved C-terminal region of the ICA69 protein (Fan et al. manuscript in preparation). It remains to be determined whether a similar molecular mechanism governs the immune reactivity against the N-terminal or the C-terminal regions of ICA69 and whether they co-exist in the same human subject.

Of particular note, the endocrine organ most severely impacted in ICA69$^{del/wt}$ and the Aire-ΔICA69 mice is the thyroid gland. Symptoms in aged ICA69$^{del/wt}$ and Aire-ΔICA69 mice suggest that autoimmune thyroiditis initiated by anti-ICA69 autoimmune response can eventually result in severe hypothyroidism. Expansion of TH1-polarized, autoreactive T-cells specific to thyroglobulin was found in E14 immunized ICA69$^{del/wt}$ mice, suggesting that the progression of thyroid gland inflammation mediated by infiltrating ICA69-specific autoreactive T-cells can lead to the loss of immune tolerance against other thyroid autoantigens commonly associated with AITD. Hypothyroidism affects 5–10% of the general population with increased prevalence in older individuals and females [55,56]. The level of *Ica1* mRNA transcripts in female B6 mice is twice as high as that of males, making the thyroid glands in females more sensitive to autoantigen ICA69 mediated autoimmunity. Indeed, in our colonies of ICA69$^{del/wt}$ mice, immune cell infiltration of thyroid glands is more prevalent in females than in males (Fan et al. unpublished observation). Consistent with the mouse data, a subset of T1D patients with AITD also developed anti-ICA69 autoimmune responses (Fan et al. manuscript in preparation). Thus, our results implicate anti-ICA69 immunity in the development of AITD in T1D patients as well as in the general population. The presence of either humoral or cellular response to ICA69 could then potentially serve as a bio-marker to predict AITD progression at early stages of T1D in clinical practice.

Our data provide further experimental support for the “central selection hypothesis” which proposes an essential role of tissue-specific antigens (TSAs) ectopically expressed in the

thymus in the negative selection of TSA-reactive thymocytes and in establishing immune tolerance to peripheral tissues [9,24,57]. Aire-ΔICA69 mice spontaneously developed insulitis, sialadenitis, thyroiditis and gastritis, with various degrees of clinical or subclinical symptoms of T1D, PSS, AITD and autoimmune gastritis, respectively. Thus, defective thymic expression of a single molecule (ICA69) seems to be sufficient to induce an autoimmune response to multiple organs. Furthermore, Aire-ΔICA69 mice are on the C57BL/6 genetic background, which carries the autoimmune diabetes resistant H-2^b MHC allele, suggesting a dominant role of TSA expression in mTECs in regulating autoreactive thymocyte negative selection. An alternative, and yet not mutual exclusive explanation for the multi-organ autoimmunity observed in Aire-ΔICA69 mice is that the loss of ICA69 expression in mTECs results in defective selection of ICA69-specific Tregs. Tregs play an important role in autoimmune diseases; lack of ICA69-specific Tregs might compromise the suppressive function of Tregs against the action of ICA69-reactive effector T-cells in Aire-ΔICA69 mice, resulting in lymphocytic infiltration in multiple ICA69-expressing organs. Indeed, previously studies have implicated a role of self-antigen expression in TECs in Treg induction [58]. At present, our results cannot differentiate these two effects.

The phenotype observed in Aire-ΔICA69 mice is reminiscent of human APS. Unlike the mouse *Ins2* gene and other *Aire*-regulated TSAs, thymic ICA69 expression in mTECs is not negatively affected by *Aire* deficiency [23]. These results suggest that thymic central tolerance of ICA69 is *Aire*-independent, and that anti-ICA69 autoimmunity might not be a major contributing factor for the development of APS1, yet might be extremely important for APS 2&3. The etiopathogenesis of human APS 2&3 remains elusive, largely due to the complexity of the diseases and the lack of suitable animal models [59]. As well, little is known about the molecular mechanisms underlying the clinical observation that patients with organ-specific autoimmune diseases have significant high risk to develop autoimmune disorders affecting other endocrine/ exocrine glands [60,61]. Although a number of genetic factors, such as the human leukocyte antigen (HLA), cytotoxic Tlymphocyte antigen 4 (CTLA-4), and protein tyrosine phosphatase non-receptor type 22 (PTPN22), have been implicated as shared susceptibility genes for multiple autoimmune disorders (e.g. T1D, AITD, CD, as well as APS 2&3), all of them modulate immunity in a systemic manner [62,63]. Far less is known about the pathogenic autoantigens determining the specificity of the tissues affected. With three different animal models, the ICA69 C-terminal peptides immunization NOD model, the heterozygous ICA69 deficient (B6.ICA69$^{del/wt}$) model, and the ICA69 thymus-specific deletion model (B6.Aire-ΔICA69) model, we demonstrated in this study that immune reactivity against the putative T1D autoantigen, ICA69, is sufficient to initiate and propagate inflammation in multiple ICA69-expressing tissues, leading to symptoms resembling human APS 2&3. Thus, ICA69 is proposed as a potential autoantigen in the pathogenesis of human APS 2&3, and immune reactivity against ICA69 could underlie the constellation of organ-specific autoimmune disorders. We propose that our animal models will be useful to facilitate further investigation of the pathogenesis of human APS 2&3.

In summary, our results suggest a possible role of anti-ICA69 immunity in the progression of secondary autoimmune disorders in T1D patients, as well as the pathogenesis of APS

2&3 and other multi-organ autoimmune disorders. Early detection of anti-ICA69 immune reactivity in patients might allow clinicians to recognize and prevent insufficiency of endocrine organs prior to morbidity. Immunomodulatory protocols to re-establish immune tolerance to ICA69 might be effective antigen-specific approaches to prevent the progression of autoimmunity in patients with APS 2&3, or to protect T1D patients from developing APS 2&3-like syndromes.

Supplementary Material

Refer to Web version on PubMed Central for supplementary material.

Acknowledgments

We thank Paul Dascani, Robert Lakomy, Alex Styche, Catarina Wong and Dr. Xin Fang for their exemplary technical assistance. We also thank Dr. Nick Giannoukakis for insightful discussions and suggestions.

Funding

This study was supported by Department of Defense grant #W81XWH-09-1-0742 and the Henry Hillman Endowed Chair to M.T., and by the National Institutes of Health grant # DK53456 to M.P.

References

1. Trucco M. Regeneration of the pancreatic beta cell. J Clin Invest. 2005; 115:5–12. [PubMed: 15630433]
2. Narendran P, Estella E, Fourlanos S. Immunology of type 1 diabetes. QJM. 2005; 98:547–556. [PubMed: 15955793]
3. Triolo TM, Armstrong TK, McFann K, Yu L, Rewers MJ, Klingensmith GJ, et al. Additional autoimmune disease found in 33% of patients at type 1 diabetes onset. Diabetes Care. 2011; 34:1211–1213. [PubMed: 21430083]
4. Mohn A, Cerruto M, Iafusco D, Prisco F, Tumini S, Stoppoloni O, et al. Celiac disease in children and adolescents with type I diabetes: importance of hypoglycemia. J Pediatr Gastroenterol Nutr. 2001; 32:37–40. [PubMed: 11176322]
5. Denzer C, Karges B, Nake A, Rosenbauer J, Schober E, Schwab KO, et al. Subclinical hypothyroidism and dyslipidemia in children and adolescents with type 1 diabetes mellitus. Eur J Endocrinol/Eur Fed Endocr Soc. 2013; 168:601–608.
6. Eisenbarth GS, Gottlieb PA. Autoimmune polyendocrine syndromes. N Engl J Med. 2004; 350:2068–2079. [PubMed: 15141045]
7. Husebye ES, Anderson MS. Autoimmune polyendocrine syndromes: clues to type 1 diabetes pathogenesis. Immunity. 2010; 32:479–487. [PubMed: 20412758]
8. Nagamine K, Peterson P, Scott HS, Kudoh J, Minoshima S, Heino M, et al. Positional cloning of the APECED gene. Nat Genet. 1997; 17:393–398. [PubMed: 9398839]
9. Anderson MS, Venanzi ES, Klein L, Chen Z, Berzins SP, Turley SJ, et al. Projection of an immunological self shadow within the thymus by the aire protein. Science. 2002; 298:1395–1401. [PubMed: 12376594]
10. Mathis D, Benoist C. Aire Annu Rev Immunol. 2009; 27:287–312. [PubMed: 19302042]
11. Seach N, Ueno T, Fletcher AL, Lowen T, Mattesich M, Engwerda CR, et al. The lymphotoxin pathway regulates Aire-independent expression of ectopic genes and chemokines in thymic stromal cells. J Immunol. 2008; 180:5384–5392. [PubMed: 18390720]
12. Kyewski B, Klein L. A Central role for Central tolerance. Annu Rev Immunol. 2006; 24:571–606. [PubMed: 16551260]

13. Pietropaolo M, Castano L, Babu S, Buelow R, Kuo YL, Martin S, et al. Islet cell autoantigen 69 kD (ICA69). Molecular cloning and characterization of a novel diabetes-associated autoantigen. J Clin Invest. 1993; 92:359–371. [PubMed: 8326004]
14. Miyazaki I, Gaedigk R, Hui MF, Cheung RK, Morkowski J, Rajotte RV, et al. Cloning of human and rat p69 cDNA, a candidate autoimmune target in type 1 diabetes. Biochim Biophys Acta. 1994; 1227:101–104. [PubMed: 7918678]
15. Friday RP, Pietropaolo SL, Profozich J, Trucco M, Pietropaolo M. Alternative core promoters regulate tissue-specific transcription from the autoimmune diabetes-related ICA1 (ICA69) gene locus. J Biol Chem. 2003; 278:853–863. [PubMed: 12409289]
16. Lemaire K, Ravier MA, Schraenen A, Creemers JWM, Van de Plas R, Granvik M, et al. Insulin crystallization depends on zinc transporter ZnT8 expression, but is not required for normal glucose homeostasis in mice. Proc Natl Acad Sci. 2009; 106:14872–14877. [PubMed: 19706465]
17. Lieberman SM, Evans AM, Han B, Takaki T, Vinnitskaya Y, Caldwell JA, et al. Identification of the beta cell antigen targeted by a prevalent population of pathogenic CD8+ T cells in autoimmune diabetes. Proc Natl Acad Sci U S A. 2003; 100:8384–8388. [PubMed: 12815107]
18. Eisenbarth GS, Jackson RA, Pugliese A. Insulin autoimmunity: the rate limiting factor in pre-type I diabetes. J Autoimmun. 1992; (5 Suppl. A):241–246. [PubMed: 1503616]
19. Cao M, Mao Z, Kam C, Xiao N, Cao X, Shen C, et al. PICK1 and ICA69 control insulin granule trafficking and their deficiencies Lead to impaired glucose tolerance. PLoS Biol. 2013; 11:e1001541. [PubMed: 23630453]
20. Holst B, Madsen KL, Jansen AM, Jin C, Rickhag M, Lund VK, et al. PICK1 deficiency impairs secretory vesicle biogenesis and leads to growth retardation and decreased glucose tolerance. PLoS biol. 2013; 11:e1001542. [PubMed: 23630454]
21. Kyewski B, Peterson P. Aire, master of many trades. Cell. 2010; 140:24–26. [PubMed: 20085700]
22. Mathews CE, Pietropaolo SL, Pietropaolo M. Reduced thymic expression of islet antigen contributes to loss of self-tolerance. Ann N Y Acad Sci. 2003; 1005:412–417. [PubMed: 14679103]
23. Bonner SM, Pietropaolo SL, Fan Y, Chang Y, Sethupathy P, Morran MP, et al. Sequence variation in promoter of Ica1 gene, which encodes protein implicated in type 1 diabetes, causes transcription factor autoimmune regulator (AIRE) to increase its binding and down-regulate expression. J Biol Chem. 2012; 287:17882–17893. [PubMed: 22447927]
24. Fan Y, Rudert WA, Grupillo M, He J, Sisino G, Trucco M. Thymus-specific deletion of insulin induces autoimmune diabetes. EMBO J. 2009; 28:2812–2824. [PubMed: 19680229]
25. Song A, Winer S, Tsui H, Sampson A, Pasceri P, Ellis J, et al. Deviation of islet autoreactivity to cryptic epitopes protects NOD mice from diabetes. Eur J Immunol. 2003; 33:546–555. [PubMed: 12645954]
26. Winer S, Astsaturov I, Cheung R, Tsui H, Song A, Gaedigk R, et al. Primary Sjögren's syndrome and deficiency of ICA69. Lancet. 2002; 360:1063–1069. [PubMed: 12383988]
27. Winer S, Tsui H, Lau A, Song A, Li X, Cheung RK, et al. Autoimmune islet destruction in spontaneous type 1 diabetes is not beta-cell exclusive. Nat Med. 2003; 9:198–205. [PubMed: 12539039]
28. Winer S, Astsaturov I, Gaedigk R, Hammond-McKibben D, Pilon M, Song A, et al. ICA69(null) nonobese diabetic mice develop diabetes, but resist disease acceleration by cyclophosphamide. J Immunol. 2002; 168:475–482. [PubMed: 11751995]
29. Budarf ML, Goyette P, Boucher G, Lian J, Graham RR, Claudio JO, et al. A targeted association study in systemic lupus erythematosus identifies multiple susceptibility alleles. Genes Immun. 2011; 12:51–58. [PubMed: 20962850]
30. Fan Y, Menon RK, Cohen P, Hwang D, Clemens T, DiGirolamo DJ, et al. Liver-specific deletion of the growth hormone receptor reveals essential role of growth hormone signaling in hepatic lipid metabolism. J Biol Chem. 2009; 284:19937–19944. [PubMed: 19460757]
31. Roescher N, Lodde BM, Vosters JL, Tak PP, Catalan MA, Illei GG, et al. Temporal changes in salivary glands of non-obese diabetic mice as a model for Sjogren's syndrome. Oral Dis. 2012; 18:96–106. [PubMed: 21914088]

32. Greenspan JS, Daniels TE, Talal N, Sylvester RA. The histopathology of Sjogren's syndrome in labial salivary gland biopsies. Oral Surg Oral Med Oral Pathol. 1974; 37:217–229. [PubMed: 4589360]
33. Helmberg W. Bioinformatic databases and resources in the public domain to aid HLA research. Tissue Antigens. 2012; 80:295–304. [PubMed: 22994154]
34. Rammensee H, Bachmann J, Emmerich NP, Bachor OA, Stevanovic S. SYFPEI-THI: database for MHC ligands and peptide motifs. Immunogenetics. 1999; 50:213–219. [PubMed: 10602881]
35. Lee IF, Qin H, Trudeau J, Dutz J, Tan R. Regulation of autoimmune diabetes by complete Freund's adjuvant is mediated by NK cells. J Immunol. 2004; 172:937–942. [PubMed: 14707066]
36. Pilon M, Peng XR, Spence AM, Plasterk RH, Dosch HM. The diabetes autoantigen ICA69 and its Caenorhabditis elegans homologue, ric-19, are conserved regulators of neuroendocrine secretion. Mol Biol Cell. 2000; 11:3277–3288. [PubMed: 11029035]
37. Lodde BM, Mineshiba F, Kok MR, Wang J, Zheng C, Schmidt M, et al. NOD mouse model for Sjogren's syndrome: lack of longitudinal stability. Oral Dis. 2006; 12:566–572. [PubMed: 17054769]
38. Jonsson MV, Delaleu N, Brokstad KA, Berggreen E, Skarstein K. Impaired salivary gland function in NOD mice: association with changes in cytokine profile but not with histopathologic changes in the salivary gland. Arthritis Rheum. 2006; 54:2300–2305. [PubMed: 16802370]
39. Robinson CP, Yamachika S, Bounous DI, Brayer J, Jonsson R, Holmdahl R, et al. A novel NOD-derived murine model of primary Sjogren's syndrome. Arthritis Rheum. 1998; 41:150–156. [PubMed: 9433880]
40. Chentoufi AA, Polychronakos C. Insulin expression levels in the thymus modulate insulin-specific autoreactive T-cell tolerance: the mechanism by which the IDDM2 locus may predispose to diabetes. Diabetes. 2002; 51:1383–1390. [PubMed: 11978634]
41. Mannisto T, Vaarasmaki M, Pouta A, Hartikainen AL, Ruokonen A, Surcel HM, et al. Thyroid dysfunction and autoantibodies during pregnancy as predictive factors of pregnancy complications and maternal morbidity in later life. J Clin Endocrinol Metab. 2010; 95:1084–1094. [PubMed: 20080846]
42. Martin AP, Marinkovic T, Canasto-Chibuque C, Latif R, Unkeless JC, Davies TF, et al. CCR7 deficiency in NOD mice leads to thyroiditis and primary hypothyroidism. J Immunol. 2009; 183:3073–3080. [PubMed: 19675158]
43. Yu L, Boulware DC, Beam CA, Hutton JC, Wenzlau JM, Greenbaum CJ, et al. Zinc transporter-8 autoantibodies improve prediction of type 1 diabetes in relatives positive for the standard biochemical autoantibodies. Diabetes Care. 2012; 35:1213–1218. [PubMed: 22446173]
44. Steck AK, Johnson K, Barriga KJ, Miao D, Yu L, Hutton JC, et al. Age of islet autoantibody appearance and mean levels of insulin, but not GAD or IA-2 autoantibodies, predict age of diagnosis of type 1 diabetes: diabetes autoimmunity study in the young. Diabetes Care. 2011; 34:1397–1399. [PubMed: 21562325]
45. Pietropaolo M, Yu S, Libman IM, Pietropaolo SL, Riley K, LaPorte RE, et al. Cytoplasmic islet cell antibodies remain valuable in defining risk of progression to type 1 diabetes in subjects with other islet autoantibodies. Pediatr Diabetes. 2005; 6:184–192. [PubMed: 16390386]
46. Verge CF, Gianani R, Kawasaki E, Yu L, Pietropaolo M, Jackson RA, et al. Prediction of type I diabetes in first-degree relatives using a combination of insulin, GAD, and ICA512bdc/IA-2 autoantibodies. Diabetes. 1996; 45:926–933. [PubMed: 8666144]
47. Grupillo M, Gualtierotti G, He J, Sisino G, Bottino R, Rudert WA, et al. Essential roles of insulin expression in Aire+ tolerogenic dendritic cells in maintaining peripheral self-tolerance of islet beta-cells. Cell Immunol. 2012; 273:115–123. [PubMed: 22297234]
48. Scaglia L, Cahill CJ, Finegood DT, Bonner-Weir S. Apoptosis participates in the remodeling of the endocrine pancreas in the neonatal rat. Endocrinology. 1997; 138:1736–1741. [PubMed: 9075738]
49. Trudeau JD, Dutz JP, Arany E, Hill DJ, Fieldus WE, Finegood DT. Neonatal beta-cell apoptosis: a trigger for autoimmune diabetes? Diabetes. 2000; 49:1–7. [PubMed: 10615942]
50. Monteiro JP, Farache J, Mercadante AC, Mignaco JA, Bonamino M, Bonomo A. Pathogenic effector T cell enrichment overcomes regulatory T cell control and generates autoimmune gastritis. J Immunol. 2008; 181:5895–5903. [PubMed: 18941178]

51. Sakaguchi S. Naturally arising CD4+ regulatory t cells for immunologic self-tolerance and negative control of immune responses. Annu Rev Immunol. 2004; 22:531–562. [PubMed: 15032588]
52. Winer S, Gunaratnam L, Astsatourov I, Cheung RK, Kubiak V, Karges W, et al. Peptide dose, MHC affinity, and target self-antigen expression are critical for effective immunotherapy of nonobese diabetic mouse prediabetes. J Immunol. 2000; 165:4086–4094. [PubMed: 11034420]
53. Karges W, Gaedigk R, Hui MF, Cheung R, Dosch HM. Molecular cloning of murine ICA69: diabetes-prone mice recognize the human autoimmuneepitope, Tep69, conserved in splice variants from both species. Biochim Biophys Acta. 1997; 1360:97–101. [PubMed: 9128175]
54. Pietropaolo M, Towns R, Eisenbarth GS. Humoral autoimmunity in type 1 diabetes: prediction, significance, and detection of distinct disease subtypes. Cold Spring Harb Perspect Med. 2012:2.
55. Rose NR. The genetics of autoimmune thyroiditis: the first decade. J Autoimmun. 2011; 37:88–94. [PubMed: 21683550]
56. Dittmar M, Kahaly GJ. Genetics of the autoimmune polyglandular syndrome type 3 variant. Thyroid. 2010; 20:737–743. [PubMed: 20578896]
57. Kyewski B, Derbinski J, Gotter J, Klein L. Promiscuous gene expression and central T-cell tolerance: more than meets the eye. Trends Immunol. 2002; 23:364–371. [PubMed: 12103357]
58. Aschenbrenner K, D'Cruz LM, Vollmann EH, Hinterberger M, Emmerich J, Swee LK, et al. Selection of Foxp3+ regulatory T cells specific for self antigen expressed and presented by Aire+ medullary thymic epithelial cells. Nat Immunol. 2007; 8:351–358. [PubMed: 17322887]
59. Michels AW, Eisenbarth GS. Autoimmune polyendocrine syndrome type 1 (APS-1) as a model for understanding autoimmune polyendocrine syndrome type 2 (APS-2). J Intern Med. 2009; 265:530–540. [PubMed: 19382992]
60. de Graaff LC, Martin-Martorell P, Baan J, Ballieux B, Smit JW, Radder JK. Long-term follow-up of organ-specific antibodies and related organ dysfunction in type 1 diabetes mellitus. Neth J Med. 2011; 69:66–71. [PubMed: 21411842]
61. Velkoska Nakova V, Krstevska B, Dimitrovski C, Simeonova S, Hadzi-Lega M, Serafimoski V. Prevalence of thyroid dysfunction and autoimmunity in pregnant women with gestational diabetes and diabetes type 1. Prilozi. 2010; 31:51–59. [PubMed: 21258277]
62. Morahan G, Mehta M, James I, Chen WM, Akolkar B, Erlich HA, et al. Tests for genetic interactions in type 1 diabetes: linkage and stratification analyses of 4,422 affected Sib-pairs. Diabetes. 2011; 60:1030–1040. [PubMed: 21266329]
63. Barrett JC, Clayton DG, Concannon P, Akolkar B, Cooper JD, Erlich HA, et al. Genome-wide association study and meta-analysis find that over 40 loci affect risk of type 1 diabetes. Nat Genet. 2009; 41:703–707. [PubMed: 19430480]

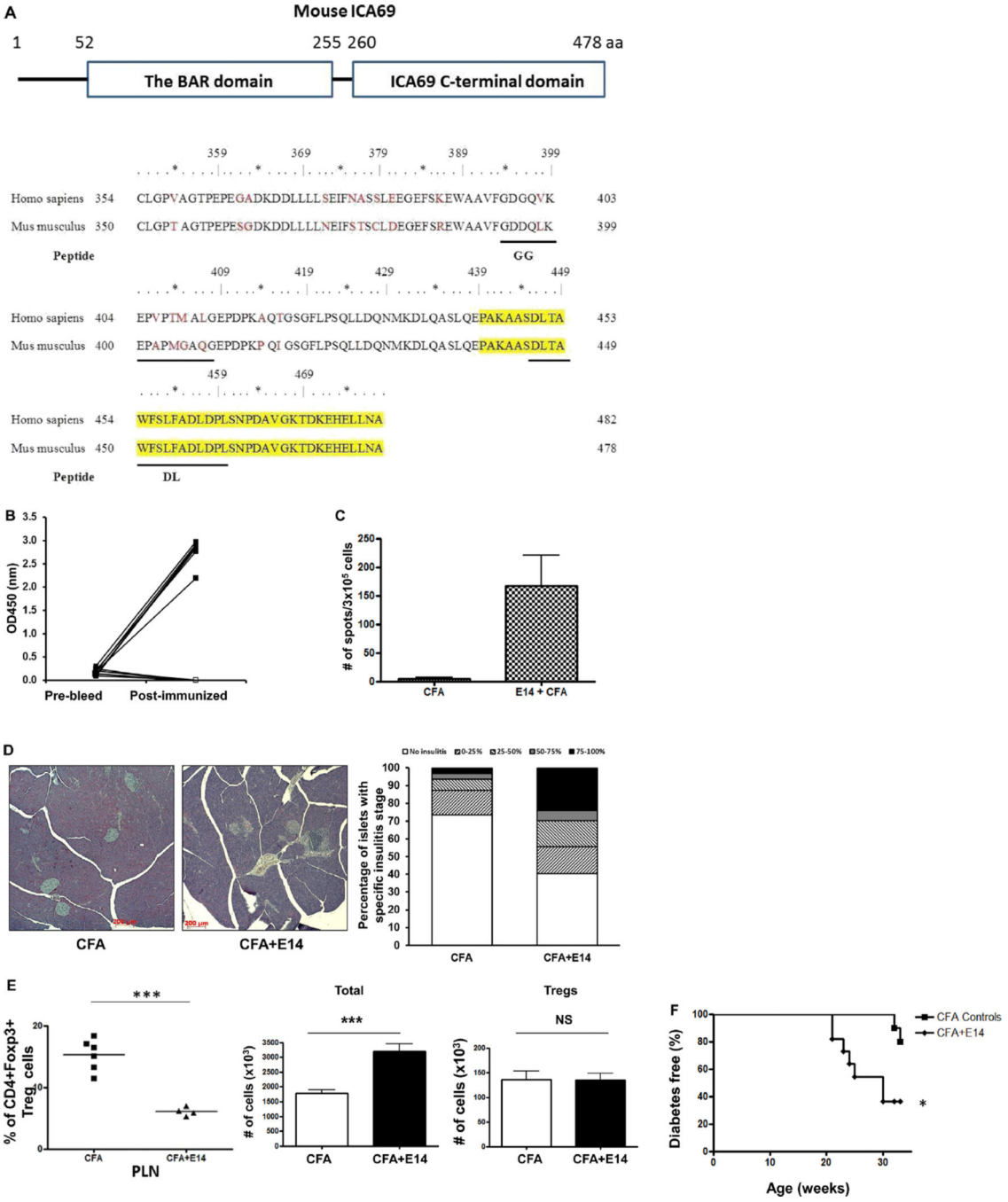

Fig. 1.

Diabetes progression in NOD mice immunized with E14 polypeptides. A. *Top panel*, schematic view of the conserved domains of the mouse ICA69 protein: the N-terminal Bin/Amphiphysin/Rvs (BAR) domain and the C-terminal ICA69 C-terminal domain (CTD). The amino acid (aa) position of each domain is listed on top. *Lower panel*, sequences of amino acids encoded by exons 13 and 14 of the mouse and human *Ica1* genes. Amino acids encoded by exon 14 are marked yellow. Other peptides used in this study (GG and DL) are underlined. B. Eight week old female NOD mice were immunized with CFA + E14 (filled-

square) or CFA alone (open-square). Serum samples were harvested 4-weeks post-immunization, and were compared to those of pre-bleed. Levels of anti-E14 seroreactivities were determined with ELISA-based, colorimetric assay. C. Eight week old female NOD mice were immunized with either CFA + E14 (n = 5) or CFA (n = 5) as controls and the presence of IFNγ-producing cells in the spleens were determined with ELISPOT 4-weeks post-immunization. Splenocytes were stimulated with E14 and the assays were run in triplicates. D. Image analysis of insulitis severity. *Left panel*, representative histological sections (H&E) of pancreata harvested from 12-weeks old NOD mice after immunization with either CFA (n = 5, left image) or CFA + E14 (n = 5, right image) for 4-weeks. *Right panel*, the degree of insulitis of each islet was assigned a score, based on the percentage of islet area occupied by infiltrates. No insulitis, 1; 0–25%, 1; 25–50%, 2; 50–75%, 3; 75–100%, 4. The bar graphs show the percentage of islets with 0–4 insulitis scores in CFA and CFA + E14 treated mice. E. Percentages of $CD4^+Foxp3^+$ T_{reg} cells in $CD4^+$ T-cells of pancreatic lymph nodes (PLN) (*left* panel) were analyzed with flow cytometry (FCM). The numbers of T_{reg} cells (*right* panel) in PLNs of E14 immunized mice (black bar, n = 4) and CFA treated controls (unfilled bar, n = 6) were calculated based on the total numbers of T-cells isolated (*middle* panel). ***, $p < 0.001$; NS, not significant. F. Diabetes progression of CFA-treated (n = 14) and CFA + E14 immunized NOD mice (n = 14). Mice were immunized at 8-weeks of age and followed till 32-weeks of age. *, $p < 0.05$.

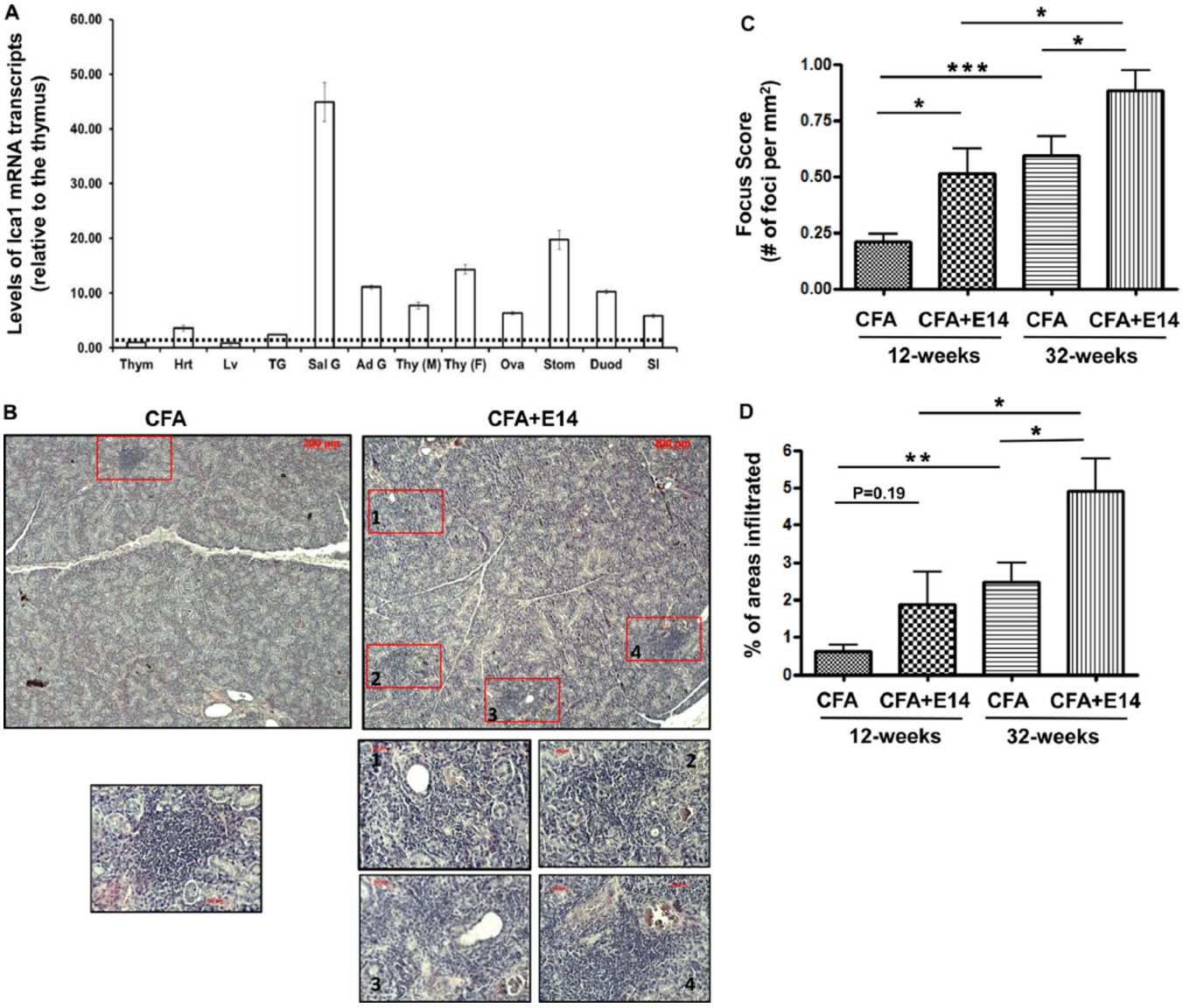

Fig. 2.

Progression of sialadenitis in NOD mice immunized with E14. A. RT-qPCR analysis of the levels of *Ica1* mRNA transcripts in various organs/tissues of C57BL/6 mice (n = 4). Thym, the thymus; Hrt, the heart; Lv, the liver; TG, the lacrimal glands; Sal G, the salivary glands; Ad G, the adrenal glands; Thy, the thyroid glands (M, males; F, females); Ova, the ovary; Stom, the stomach; Duod, the duodenum; SI, the jejunum and ileum parts of the small intestines. The relative level of *Ica1* mRNA in each organ was first normalized to the level of *Hprt* mRNA. For the ease of comparison, the relative amount of Ica1 mRNA was subsequently normalized to that of the thymus, which was arbitrarily defined as 1. B. Representative histological sections (H&E) of salivary glands harvested from 12-week old NOD mice at 4-weeks post immunization. Each lymphocytic focus is marked with unfilled red rectangle box. *Lower panels*, higher magnified images of the corresponding lymphocytic foci from the low magnified images of the *top panels*. C. Focus scores showing the number of lymphocytic focus per mm^2 of the salivary gland cross section. NOD mice were

immunized at 8-weeks of age with either CFA + E14 or CFA. Salivary glands were harvested at 12-weeks and 32-weeks of age, and process for histology. $N = 5$ for all the sample points. *, $p < 0.05$. ***, $p < 0.001$. D. Percentages of areas in the salivary glands of NOD mice infiltrated with lymphocytes. *, $p < 0.05$. **, $p < 0.01$.

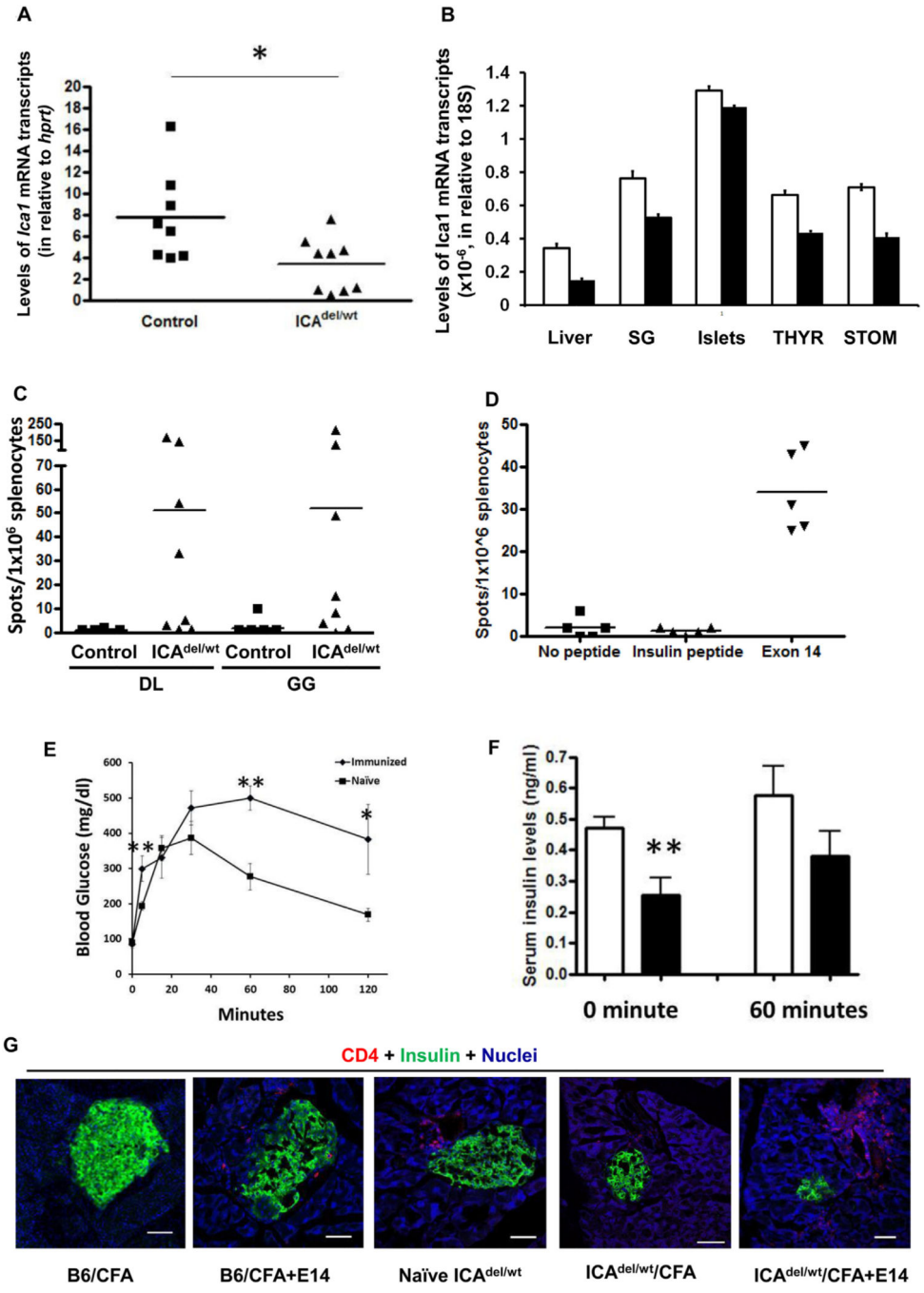

Fig. 3.

Ica1 haploid deficient mice (ICA69$^{del/wt}$) develop anti-islet autoimmunity. A. RT-qPCR analysis of *Ica1* mRNA transcript expression in CD45^{+} cell-depleted, thymic stromal cells of ICA69$^{del/wt}$ mice. Filled squares, wild-type littermate controls; filled triangles, ICA69$^{del/wt}$ thymic stroma samples. *$p < 0.05$. B. TaqMan RT-qPCR analysis of levels of Ica1 mRNA transcription in various extrathymic organs of ICA$^{del/wt}$ mice. Total RNA samples were isolated from the liver, salivary glands (SG), islets, thyroid glands (THYR) and stomach (STOM) of 12-week old ICA$^{del/wt}$ ($n = 3$, filled bar) and wild type control mice

(*n* = 3, open bar). Absolute numbers of Ica1 mRNA transcripts were calculated and normalized to those of 18S. C. ELISPOT of IFNγ-producing cells in the spleens of naïve ICA69$^{del/wt}$ mice. Splenocytes were stimulated with ICA69 C-terminal peptides GG and DL (listed in Fig. 1A). Filled squares, wild type littermate controls; filled triangles, ICA69$^{del/wt}$ mice. D. Development of anti-ICA69 autoimminity in B6.ICA69$^{del/wt}$ mice immunized with E14. ELISPOT of IFNγ-secreting splenocytes harvested from ICA69$^{del/wt}$ mice, using E14 as stimulants. An H-2^{b} restricted, insulin peptide (LWMRFLPL) was used as control. E. Intraperitoneal glucose tolerance test of ICA69$^{del/wt}$ mice immunized with exon 14 (*n* = 6), in comparison to non-immunized naïve ICA69$^{del/wt}$ mice (*n* = 6). Data are presented as mean ± SEM. *$p < 0.05$; **$p < 0.01$. F. Serum insulin levels in naïve (open bars, *n* = 7), or exon 14-immunized (filled bars, *n* = 6) mice. Sera were collected from ICA69$^{del/wt}$ mice either after overnight fasting (0 min), or 60 min after i.p. injection of a bolus of 2 g/kg of D-glucose. Data are presented as mean ± SEM. **$p < 0.01$. G. Immunohistochemistry of lymphocytic infiltration into the pancreata of E14-immunized ICA69$^{del/wt}$ mice. From left to right are representative cryosections of pancreata harvested from: B6 mice immunized with CFA, B6 mice immunized with CFA + E14 (16-weeks post immunization, only detectable in 2 out of 10 animals; not detectable in 4-weeks post treatment), naïve ICA69$^{del/wt}$ mice (24 weeks old, only detectable in 10% animals), CFA-immunized ICA69$^{del/wt}$ mice (16-weeks post treatment, detectable in 2 out 10 animals) and E14-immunized ICA69$^{del/wt}$ mice (16-weeks post treatment, detectable in majorities of the immunized animals) mice were stained with anti-CD4 (red) antibodies, and counter stained with anti-insulin (green) antibody. White arrows, infiltrating immune cells.

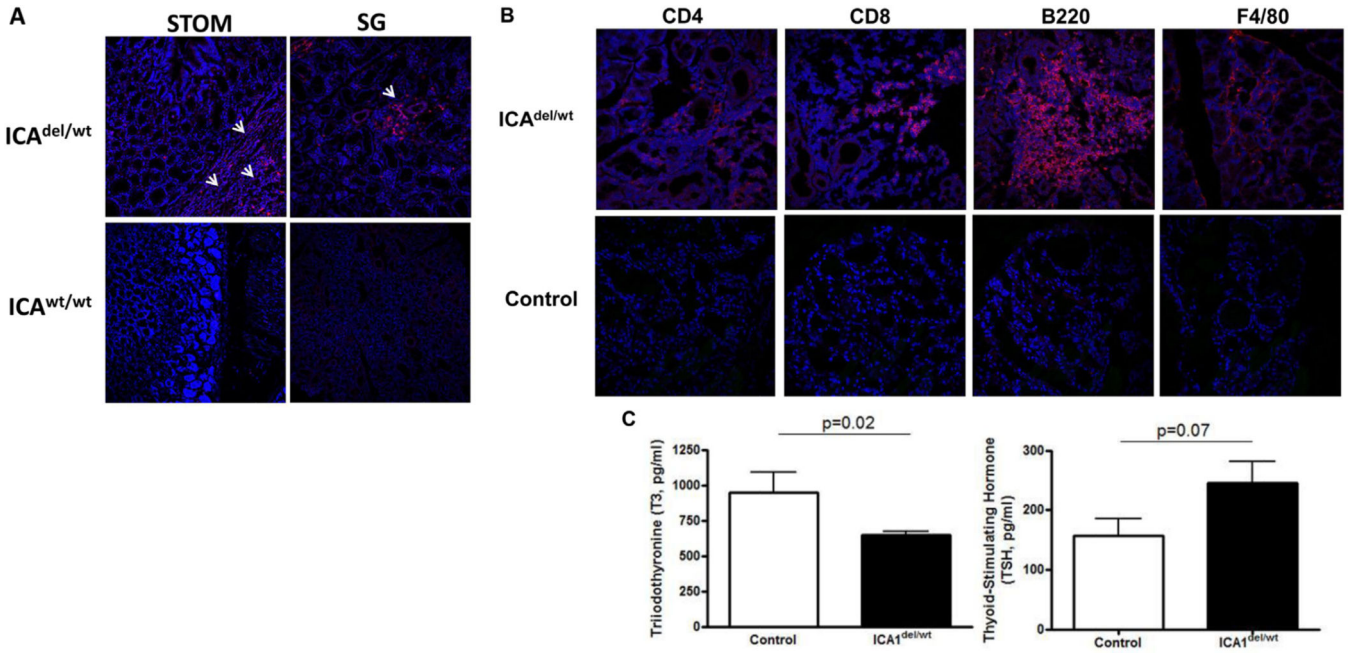

Fig. 4.

ICA69$^{del/wt}$ mice develop autoimmune thyroid disease. A. Immunohistochemistry showing lymphocytic infiltration into multiple tissues of 24-week old ICA69$^{del/wt}$ mice. Representative cryosections of stomach (STOM) and salivary glands (SG) were stained with anti-CD4 antibody (red). White arrows, infiltrating immune cells. B. Representative cryosections of thyroid glands of E14 immunized ICA69$^{del/wt}$ mice (16-weeks post immunization) were stained with anti-CD4, anti-CD8, anti-B220 and anti-F4/80 antibodies (red), showing the infiltration of CD4+ and CD8+ T-cells, B-cells and macrophages, respectively (upper panels). Age-matched wild type B6 mice immunized with E14 were used as controls (lower panels). C. Levels of thyroid hormones (total T3 and TSH) in sera of E14-immunized ICA69$^{del/wt}$ mice (filled bars, $n = 9$), in comparison to wild-type littermate controls (open bars, $n = 8$). Data were presented as mean ± SEM. p values of student t-test results were listed on top of each panel.

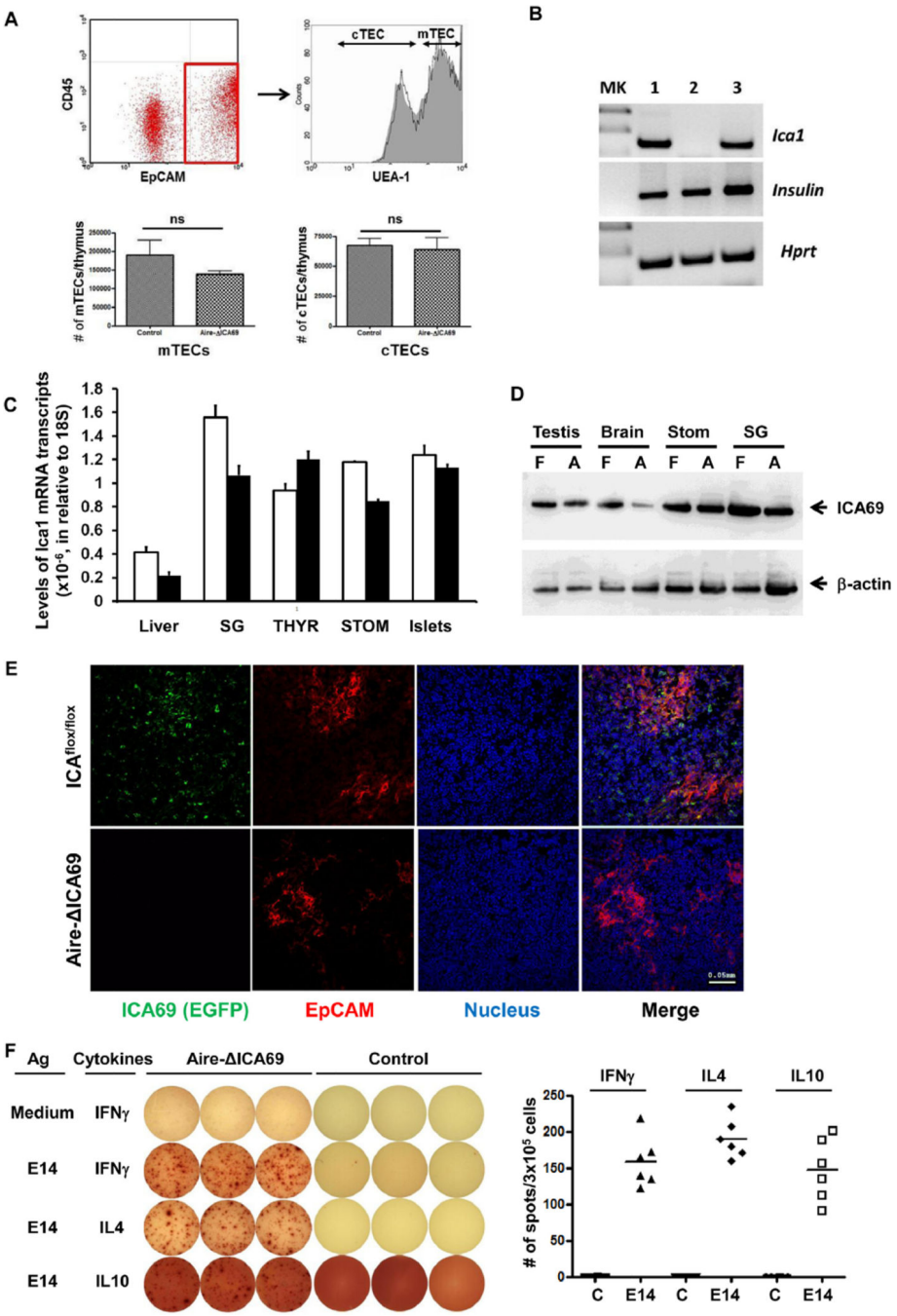

Fig. 5.

Thymus-specific deletion of the *Ica1* gene: the Aire-ΔICA69 mice. A. *Top panels*, representative dot graph of flow cytometry analysis of TECs harvested from Aire-ΔICA69 mice. EpCAM^{+}CD45^{-} TECs (within the square with red outline, *left panel*) were further separated into UEA-1^{+} mTECs and UEA-1^{-} cTECs (*right panel*). Solid line, Aire-ΔICA69 mice; gray area, Ica1$^{flox/flox}$ controls. Lower panels show the similar numbers of mTECs and cTECs in thymi of Aire-ΔICA69 (n = 4) and control mice (n = 4). B. RT-PCR analysis of levels of *Ica1* mRNA transcripts in CD45^{-} thymic stromal cells harvested from Aire-

ΔICA69 mice (*lane 2*). Thymic stromal cells harvested from Ica1$^{flox/flox}$ (*lane 1*) and Aire-Cre:Ica1$^{flox/wt}$ (*lane 3*) mice were used as controls. MK, molecular marker lane. C. TaqMan RT-qPCR analysis of levels of Ica1 mRNA transcription in various extrathymic organs of Aire-ΔICA69 mice. Total RNA samples were isolated from the liver, salivary glands (SG), islets, thyroid glands (THYR) and stomach (STOM) of 16-week old Aire-ICA69 (pooled from $n = 3$, filled bar) and ICA$^{flox/flox}$ control mice ($n = 3$, open bar). Absolute numbers of Ica1 mRNA transcripts were calculated and normalized to those of 18S. D. Western blot analysis of ICA69 protein expression in the testes, brain, stomach (Stom) and salivary glands (SG) of 16-week old Aire-ICA69 mice (A) and littermate ICAflox/flox controls (F) with rabbit anti-C-terminal ICA69 antibodies [13,23]. E. Immunohistochemical analysis of ICA69 expression in thymic medulla. Representative cryosections of thymi harvested from either the Aire-ΔICA69 mice (lower panel), or the Ica1$^{flox/flox}$ (top panel) mice, were stained with anti-EPCAM (red) and anti-EGFP (green, for ICA69) antibodies. F. Presence of E14-reactive cells in the spleens of Aire-ΔICA69 mice. *Left panel*, representative ELISPOT images (in triplicate) showing the presence of IFNγ, IL-4 and IL-10 producing cells in responding to E14, compared to age-matched littermate ICA$^{flox/flox}$ controls. *Right panel*, the data point represents the mean number of spots per well from each Aire-ΔICA69 or control mouse tested. Levels of responses similar to ICA$^{flox/flox}$ controls were detected in Aire-Cre:ICA$^{wt/wt}$ mice (data not shown).

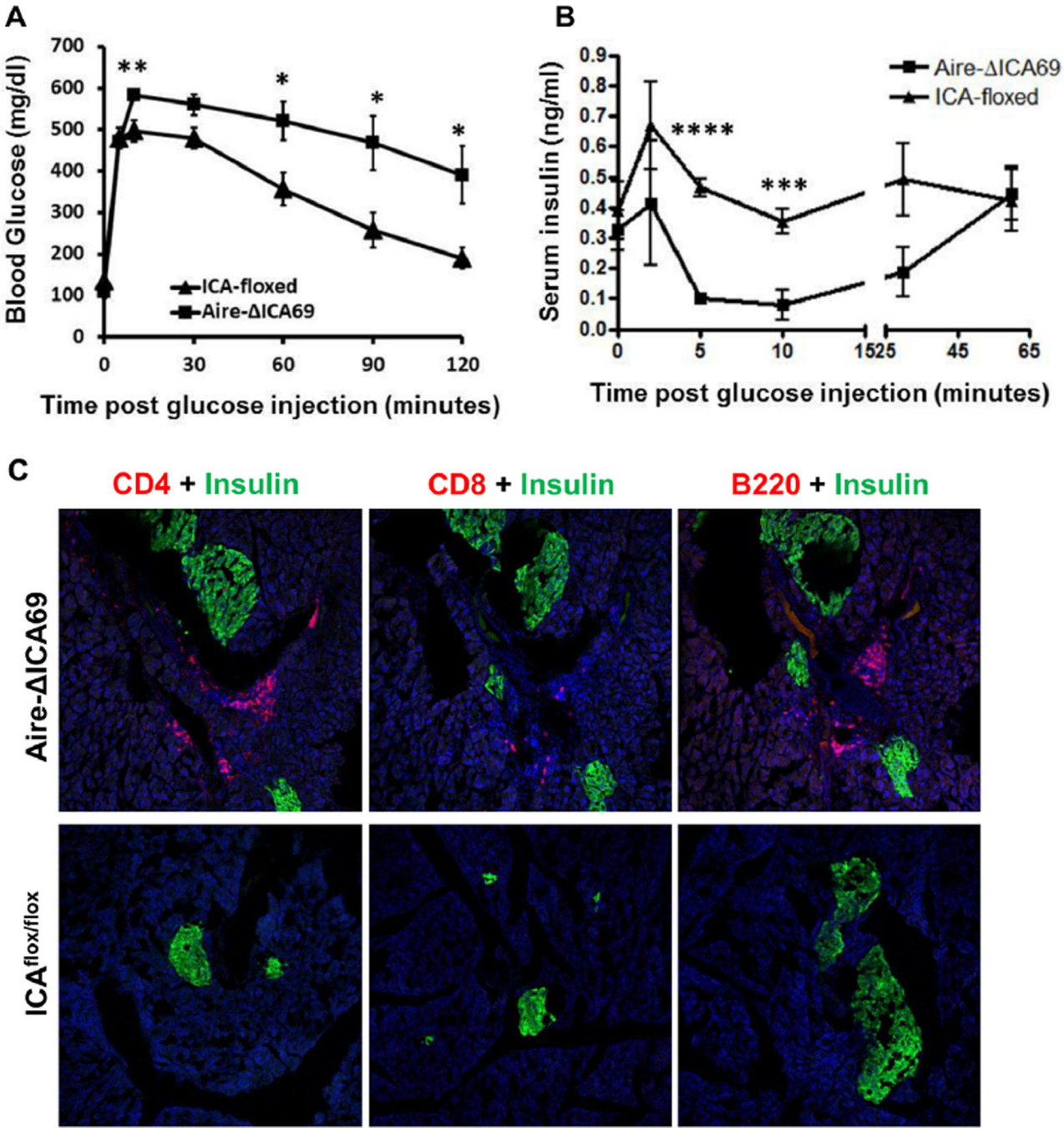

Fig. 6.

Aire-ΔICA69 mice spontaneously develop anti-islet autoimmune responses. A. Intraperitoneal glucose tolerance test. 12-week old Aire-ΔICA69 mice ($n = 7$) were challenged with a bolus of 2 g/kg D-glucose, in comparison to ICA69$^{flox/flox}$ mice ($n = 6$). Data are presented as mean ± SEM. Unpaired Student t test, *$p < 0.05$; **$p < 0.01$. B. Serum insulin levels in the Aire-ΔICA69 ($n = 7$) and the ICA69$^{flox/flox}$ ($n = 6$) mice. Sera were harvested after overnight fasting and challenged after i.p. injection of 2 g/kg of D-glucose. Data are presented as mean ± SEM. Unpaired Student t test, ***$p < 0.005$; ****$p < 0.001$.

C. Immunohistochemistry showing lymphocyte infiltration of pancreatic islets in 16-week old Aire-ΔICA69 mice. Cryosections of pancreata harvested from either the Aire-ΔICA69 (upper panel), or the $Ica1^{flox/flox}$ (lower panel) mice, were stained with anti-CD4 (red), anti-CD8 and anti-B220 antibodies and counter-stained with anti-insulin (green) antibodies. Representative images are shown.

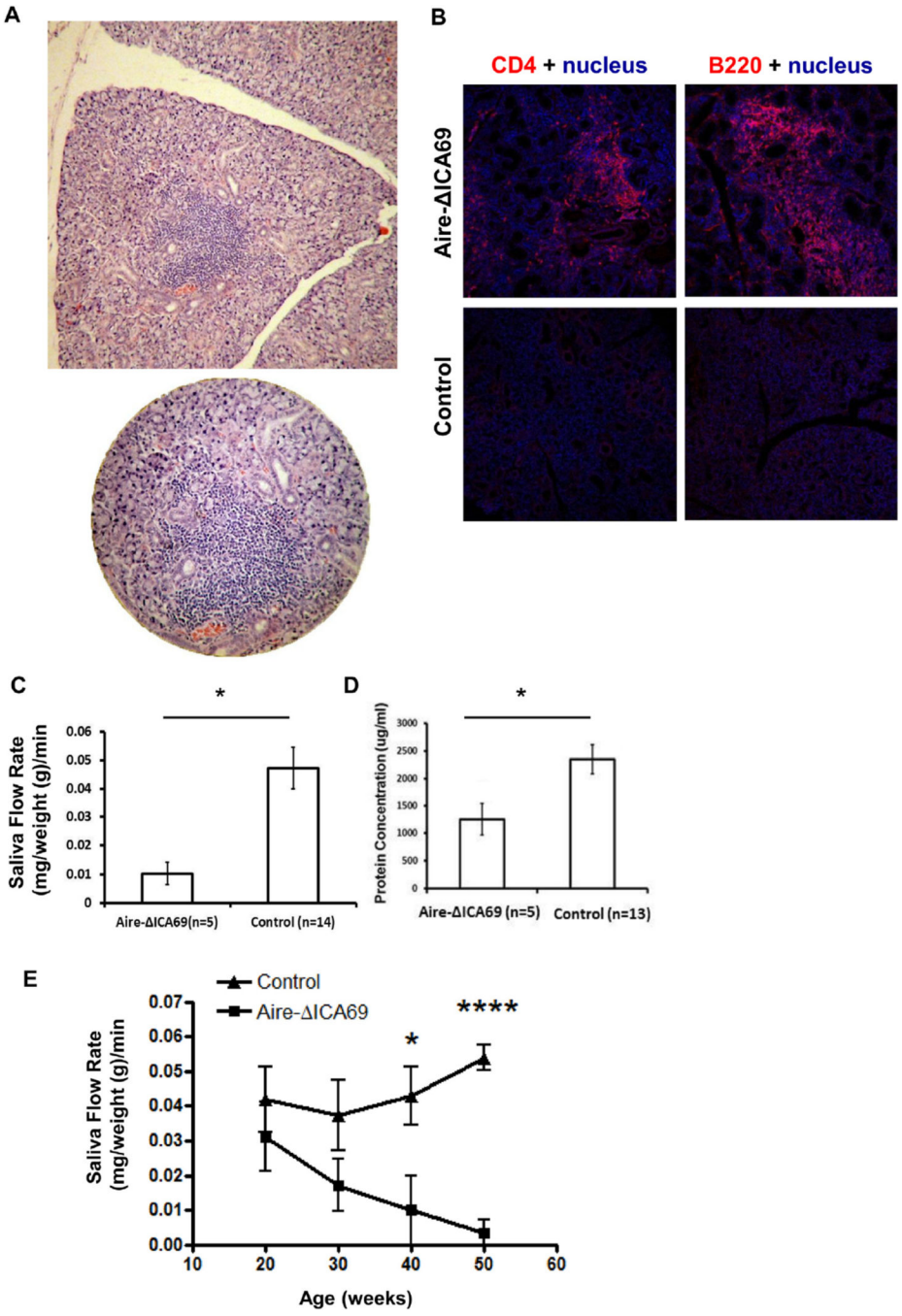

Fig. 7.

Aire-ΔICA69 mice spontaneously develop PSS. A. Representative histological sections of salivary glands harvested from 30-week old Aire-ΔICA69 mice (H&E), showing massive infiltration of immune cells. B. Immunohistochemistry showing lymphocyte infiltration of salivary glands in 8-month old Aire-ΔICA69 mice. Cryosections of salivary glands harvested from either the Aire-ΔICA69 (upper panel), or the $Ica1^{flox/flox}$ (lower panel) mice, were stained with anti-CD4 (red) and anti-B220 antibodies, and counter-stained with Hoechst 33342 (blue) for nuclei. Shown are representative images. C. Decreased saliva flow

rates in Aire-ΔICA69 mice. Aire-ΔICA69 mice (n = 5, 30–40 weeks) were anesthetized and stimulated with pilocarpine. Whole saliva was collected for 20 min. Salivary flow rate data are shown as mean ± SEM. *, $p < 0.05$. D. Decreased protein secretion in saliva of Aire-ΔICA69 mice. Data are shown as mean ± SEM. *, $p < 0.05$. E. Gradual decline of saliva flow rates in Aire-ΔICA69 along with age. Filled triangles, Aire-ΔICA69 mice (n = 3–5 per age group). Filled squares, age-matched $ICA^{flox/flox}$ controls (n = 4–5 per age group). Unpaired Student's t test, *$p < 0.05$; ****$p < 0.001$.

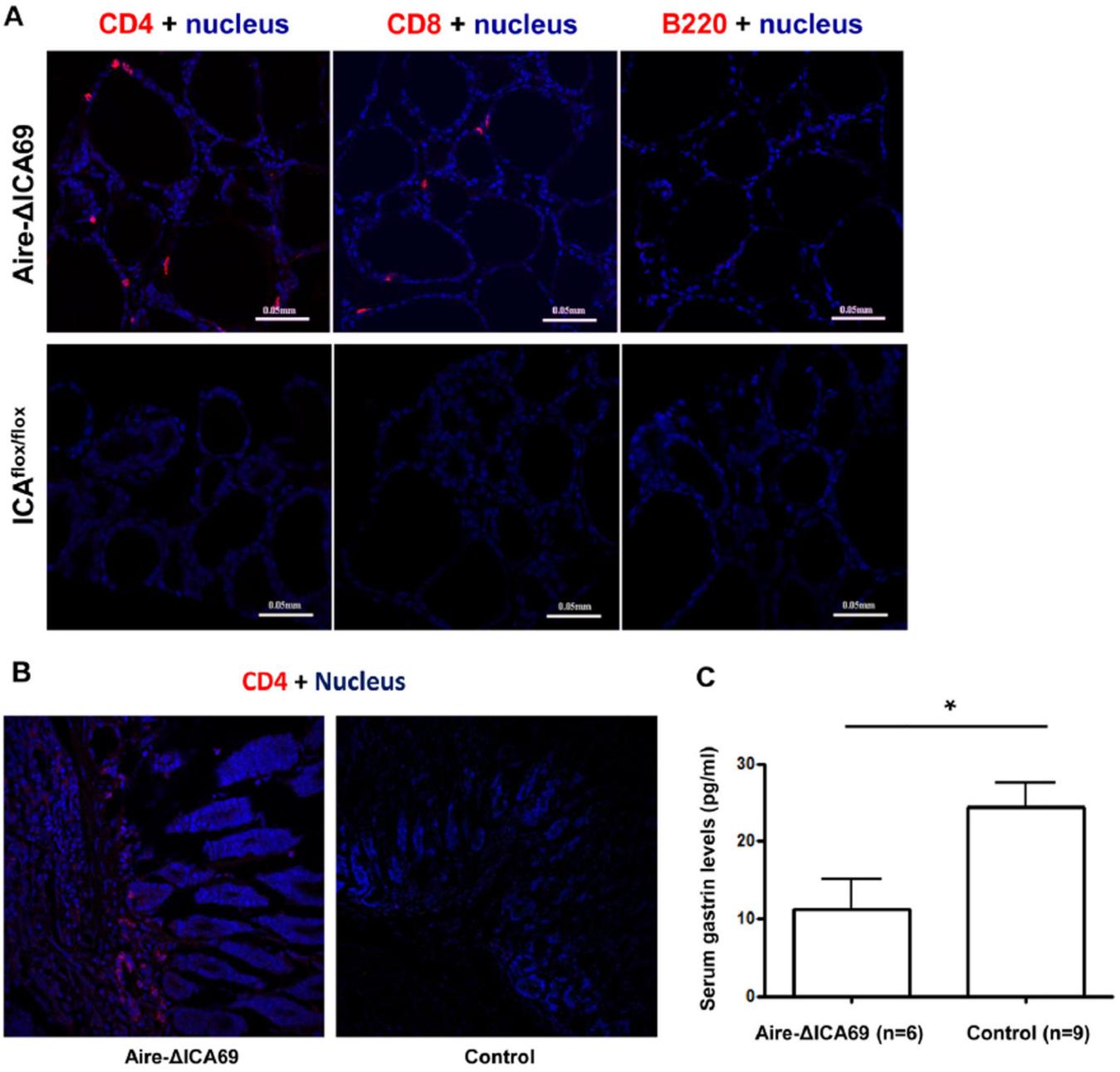

Fig. 8.

Lymphocyte infiltration in thyroid glands and the stomach of Aire-ΔICA69 mice. A. Immunohistochemical analysis of lymphocyte infiltration of thyroid glands in 8-month old Aire-ΔICA69 mice. Representative cryosections of thyroid glands harvested from either the Aire-ΔICA69 (upper panel), or the $Ica1^{flox/flox}$ (lower panel) mice, were stained with anti-CD4 (red), anti-CD8 (red) and anti-B220 (red) antibodies, and counter-stained with Hoechst 33342 (blue) for nuclei. B. Representative immunohistochemical images of stomach sections of Aire-ΔICA69 (*left* panel) and control (*right* panel) mice. Cyrosections were stained with anti-CD4 antibodies, and counter-stained with Hoechst 33342 (blue) for nuclei. C. Aire-ΔICA69 mice spontaneously developed mild gastritis. Sera were harvested from

Aire-ΔICA69 mice (20–30 weeks old, $n = 6$), and serum gastrin levels were measured with ELISA kit. Aged matched $Ica1^{flox/flox}$ mice ($n = 9$) were used as controls. *, $p < 0.05$.

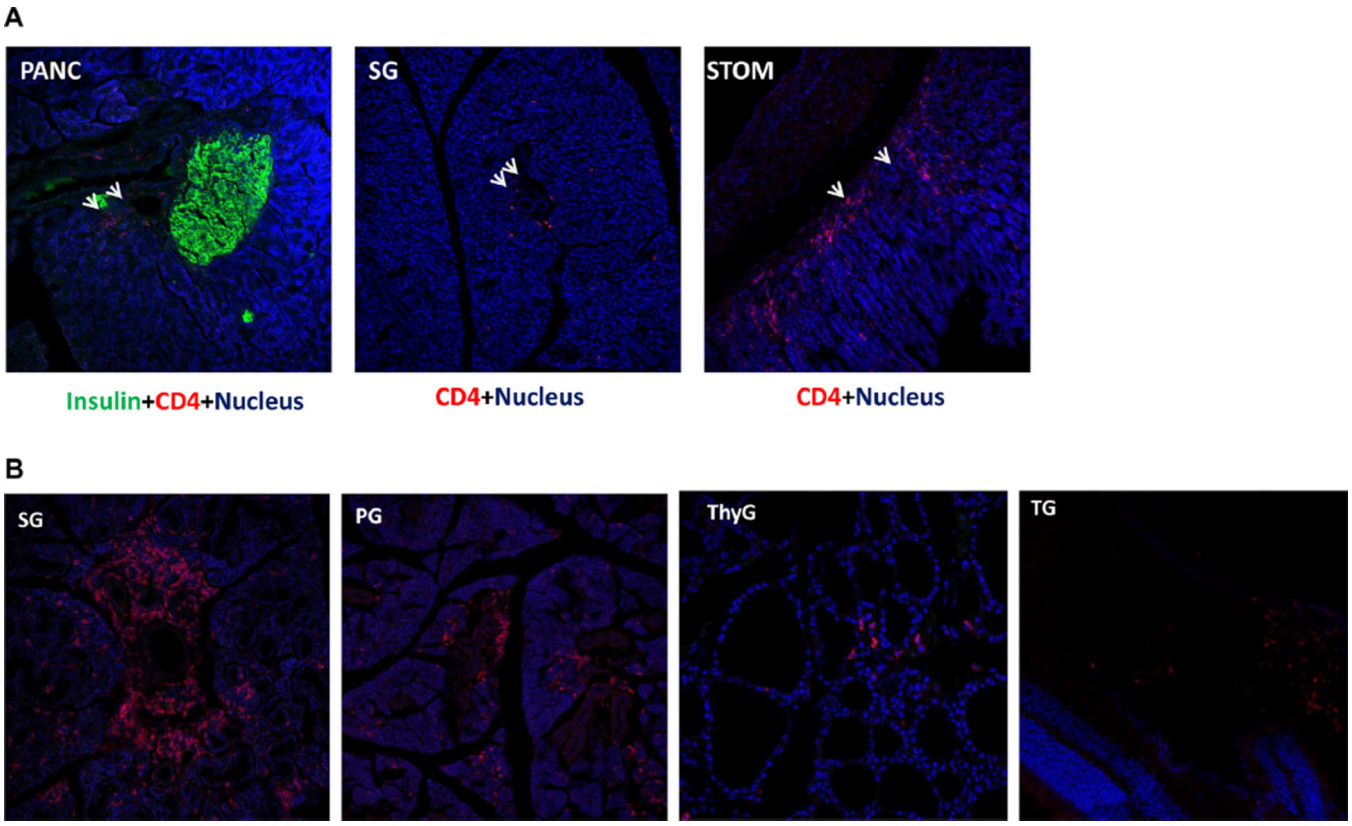

Fig. 9.

ICA69-specific autoreactive T-cells derived from Ica1 deficient thymi are sufficient to transfer multi-organ autoimmunity. A. Athymic nude mice transplanted with Ica1-deficient thymi were sacrificed at 16–24 weeks. Representative cryosections of the pancreas (PANC), the salivary glands (SG) and the stomach (STOM) were stained with anti-CD4 (red) and anti-insulin (green, for the pancreatic sections only) antibodies. No infiltrate was observed in control nude transplanted with wild type thymi (not shown). B. T-cells harvested from the Aire-ΔICA69 mice were adoptively transferred to immunocompromised Rag1−/− mice. Representative cryosections of the salivary glands (SG), parotid glands (PG), the thyroid (ThyG) and the tear glands (TG) were stained with anti-CD4 antibodies (red), and counter-stained with Hoechst 33342 (blue) for nucleus.